Cellulose
https://doi.org/10.1007/s10570-022-05011-9

ORIGINAL RESEARCH

Antioxidant activity of limonene modified cellulose pulp fiber-polylactic acid (PLA) composites

Gözde Bayer · Amirreza Shayganpour · Ilker S. Bayer

Received: 22 June 2022 / Accepted: 19 December 2022

Abstract Pulp fibers are among the most abundant and cost effective cellulose source for the fabrication of polymer-cellulose composites. A straightforward method is to impregnate pulp fibers into thermoplastic films by hot press forming. As such, tissue materials made from hard or soft wood lignin-free Kraft fibers are attractive. In this work, we prepared cellulose fiber-polylactic acid (PLA) composite films by impregnating PLA films into a 40 g/m^2 tissue paper texture. A PLA film was sandwiched between single and multiple layers of cellulose tissues by hot pressing, forming composite films. Up to 40 wt% cellulose could be incorporated into PLA in this way. The effect of cellulose fiber content on the composite thermomechanical properties has been studied and reported. A natural terpene, limonene, was infused into the cellulose fibers by immersion coating to produce antioxidant composites. Limonene-modified composites demonstrated long-term antioxidant release and activity for three days, verified by 2, 2-Diphenyl-1-picrylhydrazyl (DPPH), cupric ion reducing antioxidant capacity (CUPRAC) and free iron ions (Fe^{2+})/ferrozine chelating assays separately. The short-term (2 h) antioxidant activity of the biocomposites reached 50–70% levels depending on the cellulose fiber concentration for the DPPH and CUPRAC assays but remained lower at 20–55% levels in the metal chelating assay. Due to sustained release of limonene from the composites, at the end of the 5-day period, the iron chelating antioxidant activity of the composites improved reaching 75%, whereas for DPPH and CUPRAC assay, 90% activity was recorded. These biocomposite films can be used in active protective packaging of both food (fruit) and cosmetic products.

G. Bayer
DS Bio ve Nanoteknoloji A. Ş, Lavida City Plaza 45/7, 06530 Ankara, Turkey

A. Shayganpour · I. S. Bayer (✉)
Smart Materials, Istituto Italiano di Tecnologia, Via Morego 30, 16163 Genova, Italy
e-mail: ilker.bayer@iit.it

Published online: 26 December 2022

Graphical abstract

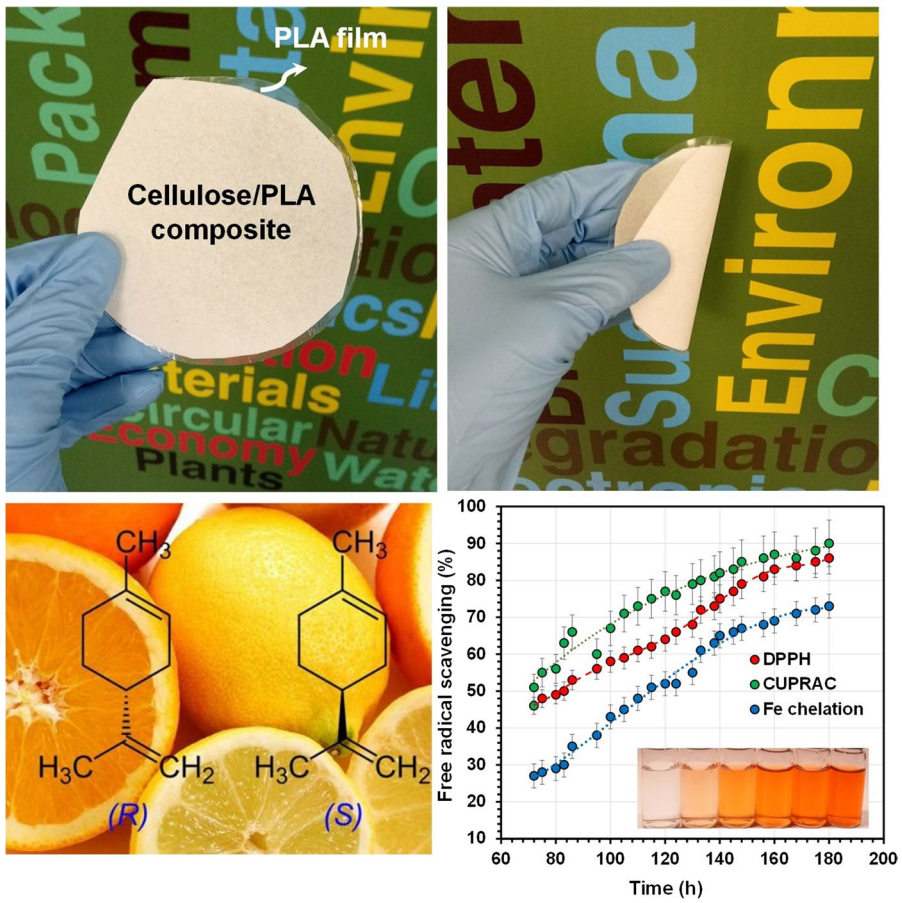

Keywords Cellulose · Paper · PLA · Limonene · Antioxidant · PLA composites

Introduction

Motivated by increasing environmental concerns related to synthetic plastic consumption, polymer composites industry has been working on replacing synthetic fibers with their natural counterparts such as cellulose-based fibers in certain reinforced plastic applications (Wright et al. 2020; Venkatarajan and Athijayamani 2021). Natural fibers, though not as strong as synthetic counterparts are abundant, can be recycled from paper products, low density, low cost, renewable, and biodegradable. Although several efficient recycling processes have been proposed and implemented in synthetic fiber-reinforced composites, including the direct structural composite recycling concept (Asmatulu et al. 2014), natural fiber reinforced polymer composites have the potential to meet the high strength-to-weight ratio for industrial production quality standards and can be utilized more and more as economic replacements (Cao et al. 2017). It must however be acknowledged that even the process of papermaking requires substantial amounts of energy and wood consumption, which contributes to larger environmental costs (Asmatulu et al. 2014; Hirn and Schennach 2015; Poletto et al. 2011; Hubbe et al. 2006; Hubbe et al. 2007). Cellulose-based natural fibers have a number of disadvantages, such as higher moisture absorption, poor thermal stability as well as lower impact strength and property variations

due to changes in the plant and crop properties and origins. Some of these drawbacks such as hydrophilicity of cellulose can be overcome by simple surface functionalization techniques including cellulose fiber functionalization with biodegradable hydrophobic monomers (Ayadi et al. 2013; Moriam et al. 2021). Cellulose is a crystalline natural polymer with a complex crystalline network structure in which allomorphs are believed to coexist in the fibril in different ratios. Particularly in the pulping process, changes can occur in the cellulose/linter structure induced by the use of certain chemical agents, temperature and pressure of the processing (Gurav et al. 2003). For instance, it was shown that in Kraft pulp, the microfibrils are more closely associated than in the sulfite pulp and holocellulose (Hirn and Schennach 2015).

Tissue paper structure is a complex system compared to other paper grades and comprises several overlapping structures like protruding fibers, crepe and fabric-based patterns at different spatial frequencies (Reitbauer et al. 2021; Ismail et al. 2020). The fiber network in a tissue paper is bonded to each other by several different forces such as inter-diffusion, mechanical interlocking, capillary forces, Coulomb forces, hydrogen bonding and Van der Waals forces (Poletto et al.; Hubbe et al. 2006). Researchers have observed significant chemical and mechanical differences among different fibers used in pulping even originating from the same tree species such as eucalypt (Pirralho et al. 2014). These differences were also reflected in the pulp fiber-thermoset polymer composites where Kraft fibers were shown to be compatible with several commercial thermoset resins such as unsaturated polyesters and vinyl esters (Du et al. 2013). Bleached soft wood Kraft fibers, bleached hardwood Kraft pulp, and unbleached softwood Kraft pulp appear to have smoother surfaces containing less non-cellulosic components such as hemicellulose, lignin, and pectin. On the other hand, bleached chemi-thermomechanial pulp and recycled pulps are richer in non-cellulosic components with rougher surface textures (Hubbe et al. 2014; Dislaire et al. 2021). Natural fiber reinforced composites require a strong interfacial adhesion between the fiber and the matrix, just as for glass-fiber reinforced composites (Sdrobiş et al. 2012). If cellulose fibers are incorporated in a hydrophobic polymer matrix without modification, due to their inherent hydophilicity, the resultant composites can have poor mechanical properties as well as increased hygroscopic character. However, very recent studies have demonstrated that functionalizing cellulose fiber surfaces with lipophilic functional compounds such as curcumin, not only eliminates this problem but also allows assembly of highly functional cellulose fiber-hydrophobic polymer composites (Quilez-Molina et al. 2021).

In certain applications such as food and drug packaging and biomedical applications, very high strength/stiffness-to-weight ratios are not required but rather other assets such as hydrophobicity, good barrier properties, and flexibility along with antioxidative and/or antimicrobial properties are sought after. In this case, cellulose pulp fibers can contribute in a positive way to the final biocomposite attributes such as enhancement in mechanical resistance (Khalil et al. 2017; Raabe et al. 2015; Peltola et al. 2019; Du et al. 2014; Saedi et al. 2021). Among bio-based and biodegradable polyesters, polylactic acid or PLA has been extensively researched in natural fiber reinforced composite applications (Zhu et al. 2020; Aumnate et al. 2021; Shen et al. 2014; Suryanegara et al. 2010). These composites feature highly appealing properties in combination with the solvent-free processes that can make them the materials of choice for several technological applications within the plastic industry including food and cosmetic packaging (Frone et al. 2016), disposable items, and toys (Singh et al. 2020), to name a few. In all of these aforementioned cellulose fiber-reinforced bio-composite applications, a number of key functionalities are very important to have such as antioxidant and antibacterial effects tethered either to PLA or cellulose polymers. Achieving these characteristics with long-lasting outcome using natural macromolecules, monomers, or extracts instead of synthetic chemicals such as butylated hydroxytoluene (BHT; an antioxidant) will eliminate complications related to food and biomedical contact approvals and biocompatibility. Although PLA-wood pulp fiber composites modified with reactive monomeric additives such as bismaleimide have been shown to feature enhanced mechanical and thermal properties, their food and medical applications are still uncertain (Baltazar-y-Jimenez and Sain 2012).

D-Limonene (4-isopropenyl-1-methylcyclohexene or limonene) is a major flavor constituent of citrus fruits. It is known to have bactericide, antioxidant, chemo-preventative and therapeutic activities, hence it is extensively used in cosmetics, foods, and other consumer products (Haque et al. 2018; Ciriminna et al. 2014; Wen et al. 2014). However, D-limonene is prone to oxidative degradation and evaporates over time just like a terpene-based solvent. It has been shown that both cellulose and PLA can uptake and encapsulate limonene allowing its sustained release and prolonging its function (Fortunati et al. 2014; Petrucci et al. 2018; Arrieta et al. 2013; Auras et al. 2006). Limonene was also shown to be an effective green plasticizer for PLA (Brüster et al. 2019; Sepúlveda et al. 2022). Since PLA is a thermoplastic, limonene can be coextruded with PLA just like a regular plasticizer and high concentrations of limonene exceeding 25 wt% can be incorporated in PLA. Untreated cellulose fibers can absorb limonene since they tend to absorb various light oils up to 30 wt. % of their weight (Rosdi et al. 2022). A household paper towel that is about 37–40 g/m^2 immersed in pure limonene would absorb about 4 times its weight of limonene within one minute. Another unique property of limonene is that it is a potent insecticide and a recent study demonstrated that cotton fabrics immersed in different ethanol solutions of limonene could be converted to very effective insect repellents with a limonene uptake range of 250 mg to 1500 mg/m^2 cotton fabric (Hebeish et al. 2008). Similarly, chitosan modified cellulose were used to encapsulate limonene and release it in a sustained manner over a period of 7 days (Lopes et al. 2019).

Even though, both cellulose (in different forms as reinforcement) and limonene (as plasticizer) have been used to modify PLA polymers to date, to the best of our knowledge no reports exist that studied limonene modified cellulose pulp fiber PLA composites. In this work, we fabricated limonene infused cellulose fiber-PLA composites utilizing a simple immersion method to modify hygiene tissue paper fibers with limonene and subsequent hot pressing different amounts of the modified tissue into PLA films. Thermo-mechanical as well as indentation hardness properties of the composites have been studied in detail and the composites demonstrated promising antioxidant activity verified by three different antioxidant assays.

Materials and methods

Materials

Hygienic paper tissues (towels) were purchased from Lucart S.p.A., Italy. According to the manufacturer, they were made from bleached soft Kraft wood pulp with a water absorbance capacity of about 6.0 g/cm^2, with a wet energy to break value of 7.0 J/m^2. The tissue papers had an apparent density of about 0.28 g/cm^3 and basis weight of about 40 g/m^2. PLA pellets with a trade name of Ingeo™ Biopolymer 4032D were purchased from Natureworks, Italy. As indicated by the manufacturer, the polymer has a melting point range of 155-170ºC and a tensile modulus of about 4.5 GPa and elongation at break value of about 7%. D-Limonene, 96.9%, MP Biomedicals grade was purchased from Fisher Scientific Italia, Italy. For antioxidant assays, analytical grade ethanol and methanol were purchased from Merck, Italy and used as received. POE (20) sorbitan monooleate (Tween80) and sodium acetate buffer solution were purchased from Merck, Italy. The free radical 2,2-diphenyl-1-picrylhydrazyl (DPPH) was purchased from Merck Italy. FerroZine(TM) iron reagent, hydrate, 98 + %, pure was purchased from ThermoFisher Scientific, Italy. Cupric chloride $CuCl_2$ (0.01 M), ferrous chloride (98% purity), 2, 9-Dimethyl-1, 10-phenanthroline (Neocuproine, assay ≥ 98%), ammonium acetate buffer solution (1.0 M, pH 7.0) were also purchased from Merck, Italy and used as received.

Sample preparation and limonene incorporation

Before preparing any samples, tissue papers were treated in a convection over at 85 °C to eliminate and minimize the adsorbed water. Papers were cut into circular disks of about 4–5 cm in diameter before limonene uptake and hot pressing with PLA. Limonene uptake with cellulose tissues was done by immersing the oven-treated (dry) tissues in limonene for three minutes. In fact, the limonene uptake saturated after 1 min of immersion and the tissues could hold up to 4 times their original weight of limonene. The concentrations of the limonene in the composites were adjusted by subsequent controlled evaporation of limonene from the saturated tissues at 50 °C (Lewczyk et al. 2020). Hot pressing powders is easier than larger sized pellets, hence PLA pellets were grinded

into a powder like consistency with an average 3 mm particle size using a Pilotina dry mill (IKA®-Werke GmbH & Co. KG, Italy). The ground powders were kept in a vacuum oven at 40 °C prior to hot pressing. PLA films were produced by hot pressing 3–4 g of milled PLA powders at 175 °C for 10 s using a hydraulic press at 1.05 MPa (TMAX-RYJ-600F, Widened Double Flatbed Heat Hydraulic Press; Germany). Upon removal from the press, the films were allowed to cool down to room temperature. The produced films had an average thickness of about 85 µm. Similarly, immersing the PLA film in pure limonene solution resulted in partial swelling of the polymer and uptake of limonene. The films saturated at about 35 wt% limonene sorption. This level was reduced to 20 wt% , 10 wt% and 5 wt% by controlled evaporation of limonene in a vacuum oven at 60 °C, a procedure similar to the one described by Arrieta et al. (2013). To produce the PLA-cellulose fiber composites, a PLA film was sandwiched between single and/or multiple layers of dry or limonene infused tissue papers and the final system was hot pressed for 10 s at 175 °C and under 2.0 MPa pressure. The final composite thickness were approximately 120 µm. No significant evaporation of infused limonene occurred during the compression that would change the limonene compositions in the composites.

Electron microscopy (SEM), atomic force microscopy (AFM) indentation and spectroscopy measurements

The morphologies of the samples were characterized by scanning electron microscopy (SEM) using a JEOL JSM-6490LA microscope (JEOL Ltd., Japan) equipped with energy dispersive spectroscopy (EDS). The surface and cross-section images were obtained by operating the SEM at 10 kV of accelerating voltage. To improve the SEM imaging quality and improve sample conductivity, the samples were coated with a 10-nm-thick gold layer with a Cressington 208HR sputter coater (Cressington Scientific Instrument Ltd). The chemical state of the composites and the pure PLA and cellulose tissue were characterized by using a single-reflection ATR accessory with a diamond crystal (MIRacle ATR, Pike Technologies) coupled to FTIR spectrophotometer (VERTEX 70v FTIR, Bruker). The spectral region scanned was 4000–600 cm^{-1} with a resolution of 4 cm^{-1}.

The nano-indentation measurements were made with by an atomic force microscope, AFM APHB-0100 (Park Scientific Instruments) operated in contact mode. A continuous stiffness measurement was followed in which a series of loading and partial unloading cycles were executed until the final indentation depth was achieved. This produced a series of hardness and modulus values as a function of indentation depth. Three different final indentation depths, namely, 30, 50, and 100 nm, were chosen with spacing between neighboring indents of 260, 400, 800, and 1600 nm, respectively avoiding plastic deformation overlapping states. Nano-indentation process involved a slow tip approach to the surface, loading and holding the tip at peak load, unloading 90% of peak load for 50 s, holding the indenter after 90% unloading for 100 s, and finally, unloading completely. An arrayed line of indents was created on every sample surface with different spacing, depending on indentation depth. Hardness (H) and elastic modulus (E) were obtained from the load–displacement data. As the indenter pierces into the sample, both elastic and plastic deformation occur while only the elastic part of the displacement is recovered during unloading. Nano-indentation hardness is calculated from:

$$H = \frac{P_{max}}{A}$$

where P_{max} is the load measured at a maximum penetration depth (h) in an indentation cycle; A is the projected contact area ($24.5 \times h_c^2$); and h_c is the contact depth of indent. The elastic modulus of the sample can be derived from the initial unloading contact stiffness (S), i.e., the slope ($\frac{dP}{dh}$) of the initial portion of the unlading curve. The relation among contact stiffness, contact area, and elastic modulus is given as:

$$S = 2\beta\sqrt{\frac{A}{\pi}}E_r$$

where β is a indenter geometry dependent constant ($\beta = 1.034$ for a Berkovich indenter) and E_r is reduced elastic modulus, which accounts for the fact that elastic deformation occurs in both the sample and the indenter. The sample elastic modulus (E_s) can then be calculated as (Oliver et al. 1992):

$$E_S = \left(1 - {\vartheta_S}^2\right)\left(\frac{1}{E_r} - \frac{1 - {\vartheta_i}^2}{E_i}\right)^{-1}$$

where ϑ_S and ϑ_i (0.07) are the Poisson's ratios of the specimen and indenter, respectively, while E_i is the modulus of the indenter (1141 GPa).

Thermomechanical characterization

The mechanical properties of the cellulose tissues were measured at 20 °C and 50% relative humidity by using the KES-FB1-A Tensile and Shear Tester (Kato Tech Co., Ltd.). It analyzes hand movements-referred to as "tensile" and "shear"-performed by artisans and professionals when judging a fabric's texture. The testing system performs these movements mechanically with varying tensile deformation rates (0.05 to 0.5 mm/s), producing numerical data. Measurable mechanical properties are tensile rigidity (LT), tensile energy (WT), tensile recoverability (RT), shear rigidity (G), elasticity for minute shear (2HG) and elasticity for large shear (2HG5). For tissue paper, extensibility, tensile energy, tensile resilience and linearity in tensile energy are typically measured. Mechanical properties of the tissue papers were measured with uniaxial tensile testing (Instron 3365 universal testing machine). Dog bone-shaped samples were cut with a gauge length of 25 mm and a width of 4 mm. Strain displacement of 20 mm min^{-1} was used. Stress–strain curves were obtained at 25 °C and 44% relative humidity (RH). At least four measurements were made for each sample and the results were averaged. The Young's modulus was calculated from the slope of the linear part of the stress–strain curve (before elastic limit, if any). Both Young's modulus and elongation at break values were calculated using the built-in software of the tensile tester. The tensile strength was measured in the warp and the weft direction.

The dynamic mechanical analysis (DMA) of the films and composites were conducted by DMA Q 800 (TA Instruments, USA). The viscoelastic behavior was performed by storage modulus and loss factor by heating from − 100 to 250 °C in a single cantilever mode with the heating rate of 5 °C/min, frequency of 1 Hz, and strain of 0.1%. The test specimen dimensions were approx. 2.0 × 5.0 × 30.0 mm (thickness × width × length). Averages from three measurements for each sample were reported. Weight changes during limonene evaporation from the samples were measured with a Kern ALS–ALJ digital balance (KERN & SOHN, Germany) with a sensitivity of 0.0001 g in an environmental chamber (KBF LQC Humidity Test Chamber, BINDER, Germany) set at 30 °C under 50% RH. TA instruments Q20 differential scanning calorimeter (DSC) measurements were performed in the temperature range from room temperature to 200 °C, at 2, 5, 10 and 20 °C min^{-1}, with two heating and one cooling scans. Melting and cold crystallization temperatures and enthalpies (T_m, T_{cc} and ΔH_m, ΔH_{cc}) were determined from the second heating scan and glass transition temperature (T_g) were also measured. The degree of crystallinity (X_{cc}) was calculated through the following equation:

$$X_c = 100\% \times \left[\frac{\Delta H_m - \Delta H_{cc}}{\Delta H_m^c}\right] \times \frac{1}{W_{PLA}}$$

where ΔH_m is the melting enthalpy, ΔH_{cc} is the cold crystallization enthalpy, ${\Delta H_m}^c$ is the melting heat associated to pure crystalline PLA (93 J g^{-1}) and W_{PLA} is the weight fraction of PLA in the composites. Tensile tests were measured on a mechanical testing equipment (Instron 2345) at 20 °C with a relative humidity (RH) of 50% and a crosshead speed of 5 mm/min. Before measuring, all the samples were conditioned in the controlled environment for at least 24 h. Rectangle shaped samples were used (1 × 5 cm^2, 70–80 m in thickness), and 10 replicates were tested to check repeatability. Water uptake and water vapor permeation measurements and procedures were identical to our previous report (Bayer et al. 2022) and will not repeated here for brevity.

Diphenylpicrylhydrazyl (DPPH) antioxidant assay

Limonene infused films were cut into 2 cm × 2 cm square coupons and were placed in clean glass vials. The vials were equipped with a magnetic stirrer. The vials were filled with a 0.2 mM solution of DPPH in methanol to a volume of 12 ml. Before sealing the vials, Tween 80 surfactant was added to a concentration of 0.1% by volume. The vials were stored in dark and ambient conditions under gentle constant magnetic stirring for 30 min. At different time intervals, 2 to 3 ml of solutions were withdrawn from the vials, transferred into a polystyrene cuvette and the solution

light absorbance was measured at 517 nm by using a Cary 6000i Scan UV–Visible spectrophotometer (Walnut Creek, CA, USA).

The CUPRAC (cupric ion reducing antioxidant capacity) measurements

The antioxidant assay was adapted from Apak et al. (2007) with minor modifications. The CUPRAC method is based on the reduction of the cupric neocuproine (Nc) complex (Cu(II)-Nc) into cuprous form (Cu(I)-Nc) by the antioxidant molecule. CUPRAC test solution used in this method is usually prepared using $CuCl_2$ such that the final concentration of Cu(II) in the solution is 10 mM, neocuproine in absolute ethanol with a concentration 7.5 mM, and 1.0 M CH_3COOH/CH_3COONH_4 buffer solution at pH = 7.0. Similar sized samples were inserted in glass vials that contained 0.5 ml Cu (II) + 0.5 ml Nc + 0.5 ml buffer + 100 ml of methanol + 0.45 ml water (with 0.1% Tween 80). The vials were sealed and magnetically stirred for 30 min in dark before sampling for light absorbance. Solutions were withdrawn at different time intervals, as described in the previous section, and were placed in the spectrophotometer to measure the absorbance at 450 nm. A mixture of CUPRAC reagent, water, and methanol without sample films was used to zero the spectrophotometer.

Metal chelating antioxidant assay

The chelating capacity of the limonene infused composites was determined based on the method by Lee et al. (2006) with minor modifications. Vials containing the composite samples were filled with 12 mL of 0.1 M sodium acetate buffer at pH = 4.9 and 0.5 mL of 2 mM iron (II) chloride. After 30 min of incubation at room temperature while mixing gently with a magnetic stirred, 0.2 mL of 5 mM ferrozine was added. After 30 min, the absorbance was measured at 562 nm. Distilled water and EDTA were used as negative control and as standard metal chelator of the assay, respectively. The percentage of inhibition of ferrozine–Fe^{2+} complex formation was calculated as $[(A_0 - A_1)/A_0] \times 100$, where A_0 was the absorbance of the negative control, and A_1 was the absorbance of the extracts. The same relation for percent inhibition calculation was used for all the antioxidant assays. All the assays were carried out in triplicate. The results were expressed as average values with their corresponding standard deviations (SD). Also in all assays, pure limonene was used as a control test. The control tests were made by simply adding limonene in the test vials such that the added amount was equivalent to the 20 wt. % limonene concentration within PLA-cellulose fiber composite with 40 wt% cellulose.

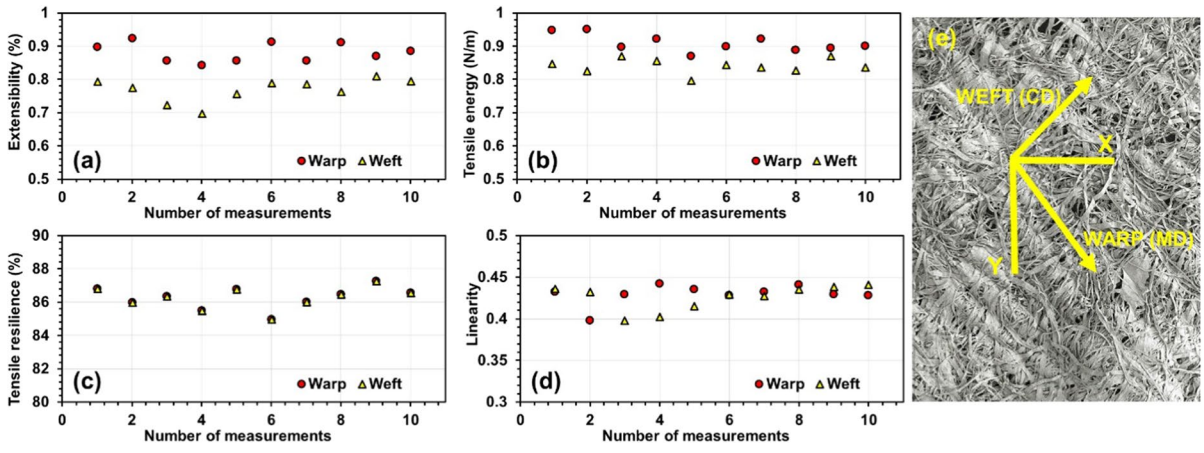

Fig. 1 KES-F, known as low stress testing measurement results for the tissue paper used in this study. **a** Percent extensibility, **b** tensile energy, **c** tensile resilience results and **d** Linearity measurements. All measurements were made in both warp and weft direction and obtained from 10 different samples. **e** SEM image of the tissue paper and the warp (machine direction, MD) and weft (cross direction, CD) directions used in the measurements

Results and discussion

Mechanical properties of the cellulose tissue

Use of cellulose pulp fibers in the production of new bio-based polymeric materials is a growing field of research and development with good future prospects (Graupner et al. 2009). However, the development of new materials containing pulp cellulose fibers requires far better mechanical properties such as improvements in extensibility in cellulose fibers. In fact, highly extensible papers can have new potentials in sustainable packaging (Vishtal et al. 2014; Kouko et al. 2020). The mechanical properties of the bleached pulp tissue papers are generally analyzed by Kawabata Evaluation System for Fabric (KES-F; low stress testing) (Kawabata et al. 2002; Lam et al. 2011). The test system allows measurement of extensibility, tensile energy, tensile resilience and linearity in tensile energy. The results are presented in Fig. 1 for both warp and weft directions. Note that since tissue paper are non-woven (see Fig. 1e), the warp and weft directions can be taken as the Yankee cylinder machine direction (warp) and the cross direction (weft) (Ismail et at. 2020). In Fig. 1a, a set of extensibility measurements are shown. Under a specific tensile stress, extensibility is the percentage of the extended length compared to the original length. In other words, it is the percentage of strain at maximum applied force (500 gf cm^{-1}). High values of extensibility indicate greater elongation of the fabric under an applied stress. For this particular cellulosic tissue, the average warp extensibility was 0.86% and average weft extensibility was found to be 0.76%. Cotton fabrics generally demonstrate extensibility values of within 5 to 9% depending on the fabric texture and the treatments applied (Lam et al. 2011; Pawlak et al. 2022).

The values reported in Fig. 1a are similar to machine direction values of a typical blotting paper (i.e., bibulous paper; absorbent paper) (Parfitt et al. 2003; Dasmohapatra et al. 2018). Figures 1b, c show measurement results of the tensile energy and resilience values. A low tensile energy value causes hard extension, while a low value of tensile resilience means inelastic behavior. According to Kawabata fiber network quality chart, a tensile resilience value between 72 and 82% indicate good processability that is important for thermoforming applications (Kojima et al. 2016).

In Fig. 3c, the average tensile resilience was found to be 86% that is somewhat outside of the bound set forth by Kawabata criteria. On the other hand, the cellulose fiber network used in this study has on average a tensile energy value of about 0.9 N/m. For instance, lignocellulosic microfibers feature tensile energy values between 5 and 10 N/m depending on the microfiber chemistry and the process history (Jahangir et al. 2020). The tensile energy values are similar to some paper towels made from recycled cellulose fibers (Dasmohapatra et al. 2018). Linearity (Fig. 1d) is inversely proportional to tensile strain in the sense that the lower the tensile strain at the same tensile load is, the higher the linearity is and this means the fiber network is more stable as it can return to its original dimensions after unloading (i.e. no plastic deformation) (Dapkūnienė et al. 2006). An average linearity value of about 0.43 was measured for the tissue paper used in this work. This value is about half of woven polyester or nylon fabrics and is in agreement with other commercial paper towels characterized in the literature (de Assis et al. 2018). The stress–strain test results of the tissue papers are

Table 1 Mechanical properties of the tissue paper measured in the machine direction (MD) and cross direction (CD). Three different elongation rates were used in each direction indicated as MD1 to MD3 and CD1 to CD3

Sample number	Tensile strength (kPa)	Young modulus (MPa)	Elongation at break (%)	Rate of elongation (%/min)
MD1	195.6 ± 6	13.6 ± 0.3	18.9 ± 0.9	15
MD2	210.3 ± 6	12.9 ± 0.3	21.0 ± 0.9	25
MD3	205.8 ± 6	13.3 ± 0.3	19.6 ± 0.9	50
CD1	120.3 ± 0.7	13.3 ± 0.6	9.2 ± 0.2	15
CD2	118.6 ± 0.7	11.9 ± 0.6	8.6 ± 0.2	25
CD3	119.5 ± 0.7	12.5 ± 0.6	8.9 ± 0.2	50

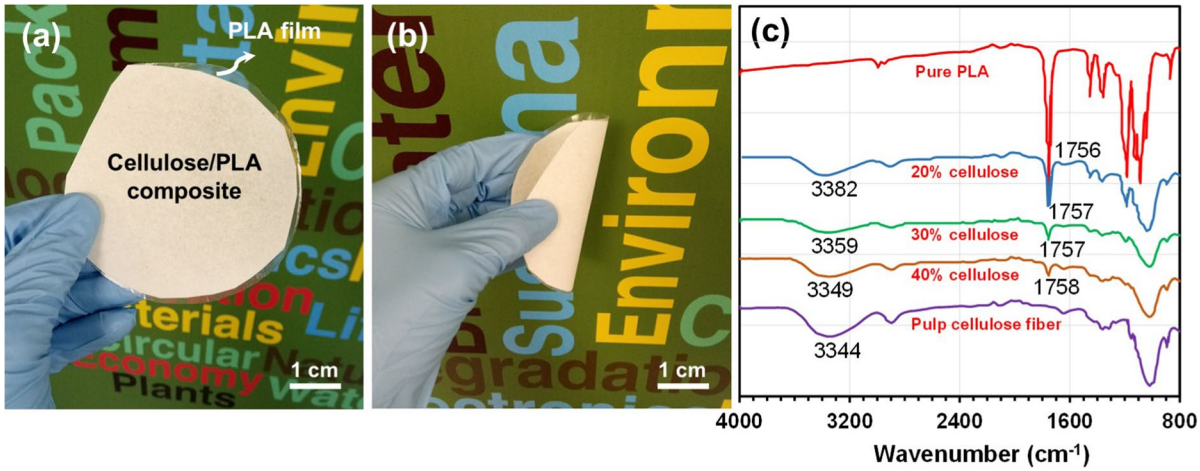

Fig. 2 **a** Photograph of a 40 wt% cellulose fiber/PLA composite produced by hot pressing the tissue paper into the PLA film. **b** Photograph of the same composite showing its ability to flex and bend. **c** FTIR spectra of pure PLA, cellulose tissue and the composites

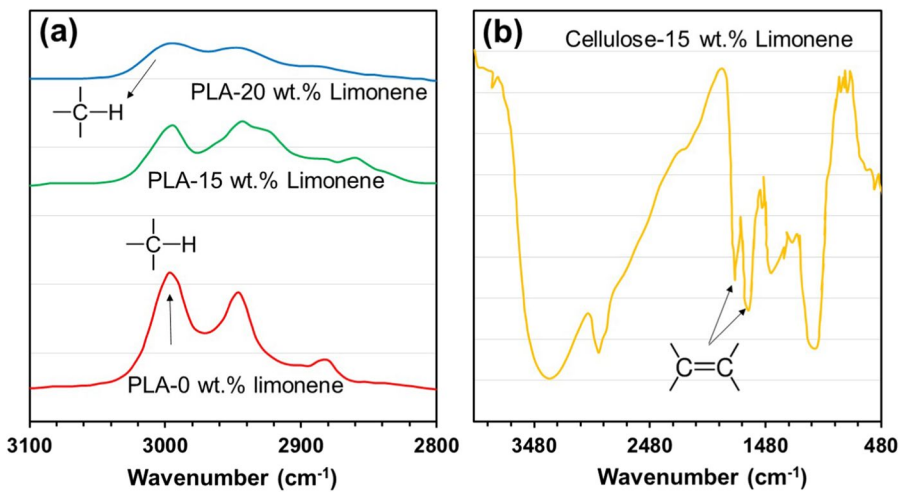

Fig. 3 **a** FTIR spectra of pure PLA, PL with 15 wt. % limonene and PLA with 20 wt% limonene. As the limonene concentration increases −CH stretching bands of PLA broaden. **b** Aromatic unsaturated bands dues to limonene in the FTIR transmittance spectrum of limonene absorbed cellulose tissue

shown in Table 1 for both machine (MD) and cross (CD) directions (see Fig. 1e) with three measurements for each direction. Tensile strength values appear to be similar with other commercial creped cellulosic hand sheets reported recently (de Assis et al. 2020; Leppänen et al. 2020). Machine direction tensile strength was about 40% higher than the cross direction. Measurements were made at three different elongation rates to investigate the effect of strain rate on mechanical properties of the cellulose fiber network and no major effect was noticed between 15 and 50%/min strain rates.

Morphology of the composites and limonene uptake

The film grade PLA polymer (NatureWorks® Ingeo™ 4032D) was hot-pressed into the texture of the cellulose tissues forming composites as shown in Fig. 2. More precisely, the PLA films were sandwiched with cellulose tissues and subsequently hot pressed. By increasing the number of ply layers, one can produce PLA/cellulose composites with varying cellulose content. Up to 40 wt% cellulose fiber/PLA composites were still flexible and bendable as shown in Fig. 2b.

The FTIR spectra of the composites shown in Fig. 2c show that the OH stretching band of the pulp cellulose fibers at 3344 cm^{-1} undergoes a blue-shift from 3344 to 3382 cm^{-1} in the composites. This may be attributed to the fact that in the presence of PLA polymer, the hydrogen bonds between the OH groups in cellulose will be partially disrupted. New hydrogen bond interactions between the H atom of the OH group in cellulose and the O atom of the C=O group in PLA would be established, possibly shortening the O–H bond in the cellulose of the composites and causing a blue shift in the stretching vibration of O–H (Moreno et al. 2020). We also postulate that compared to the aforementioned shift in the stretching vibration peak of O–H in cellulose (~33 cm^{-1}), the shift in the C=O stretching vibration peak of PLA remained practically unchanged (1–2 cm^{-1} at 1758 cm^{-1}) despite the hydrogen bond formation. This can be correlated to the stretching vibration force constant of the C=O double bond that was affected less than that of the O–H bond (Zhou et al. 2001). Figure 3a shows an FTIR region (3100–2800 cm^{-1}) spectra of pure PLA and PLA-limonene films (no cellulose). The spectrum region between 3000 and 2860 cm^{-1} is characterized by –CH stretching bands; this region shows a high absorption for PLA, with the intensities of these peaks decreasing with increase in limonene concentration. There is also a broad absorption due to the absorption of cyclohexene group at about 3000 cm^{-1} which overlap –CH peaks (Montoille et al. 2021). Figure 3b shows the FTIR spectrum of a cellulose tissue that was allowed to absorb 15wt. % limonene.

The spectrum presents the characteristic bands corresponding to cellulose with the most intense band in the high-energy region due to a large amount of OH groups of the carbohydrates. The intense band at 1045 cm^{-1} corresponds to the link C–O–H or C–O–R (alcohols or esters) while the distinctive band at 2925 cm^{-1} is related to the presence of C–H stretching vibration together with bending vibrations around 1428 cm^{-1} of aliphatic chains ($–CH_2–$ and $–CH_3–$) forming the basic structure of this polyphenol modified cellulose materials (Liu et al. 2018). The signal at 1736 cm^{-1} can be assigned to carbonyl groups presence like ester. Finally, the band at around 1617 cm^{-1} can be attributed to unsaturated aromatics due to the presence of limonene. Characteristic limonene bands were highly oppressed in cellulose/PLA/limonene composites most probably due to hydrogen bonding interactions between PLA-cellulose and the ability of limonene to establish π-hydrogen bonds with hydrophilic polymers (Rehan et al. 2018; Frank et al. 2020).

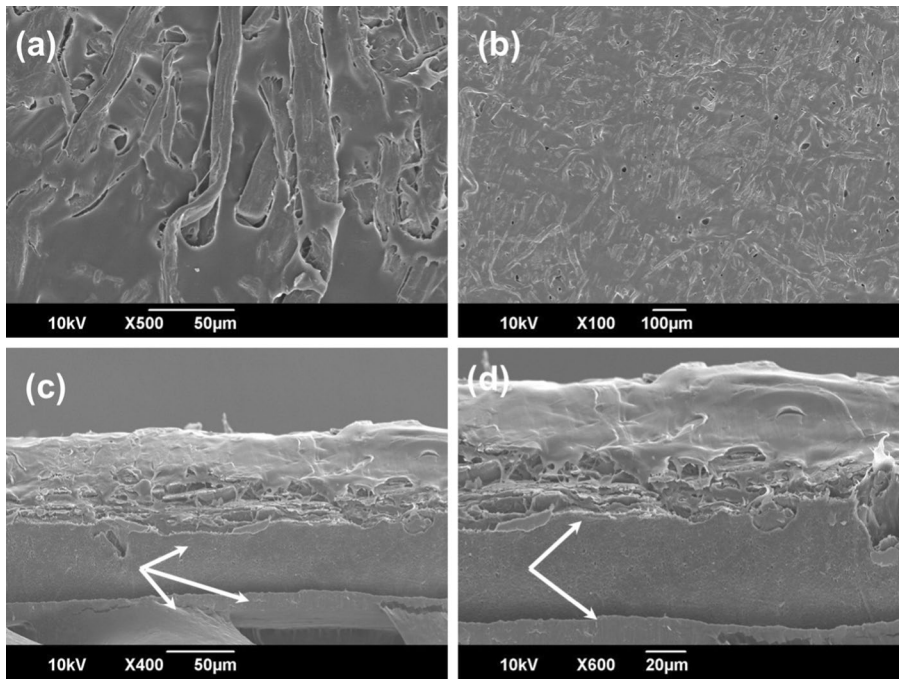

Fig. 4 Surface (**a**, **b**) and cross section (**c**, **d**) SEM micrographs of 40 wt% and 20 wt% cellulose fiber-PLA composites. In the cross section images, the "spillover" thin PLA layer is due to cutting of the specimens. The white arrows indicate the conductive adhesive tape used to fix the specimens on the SEM sample mount

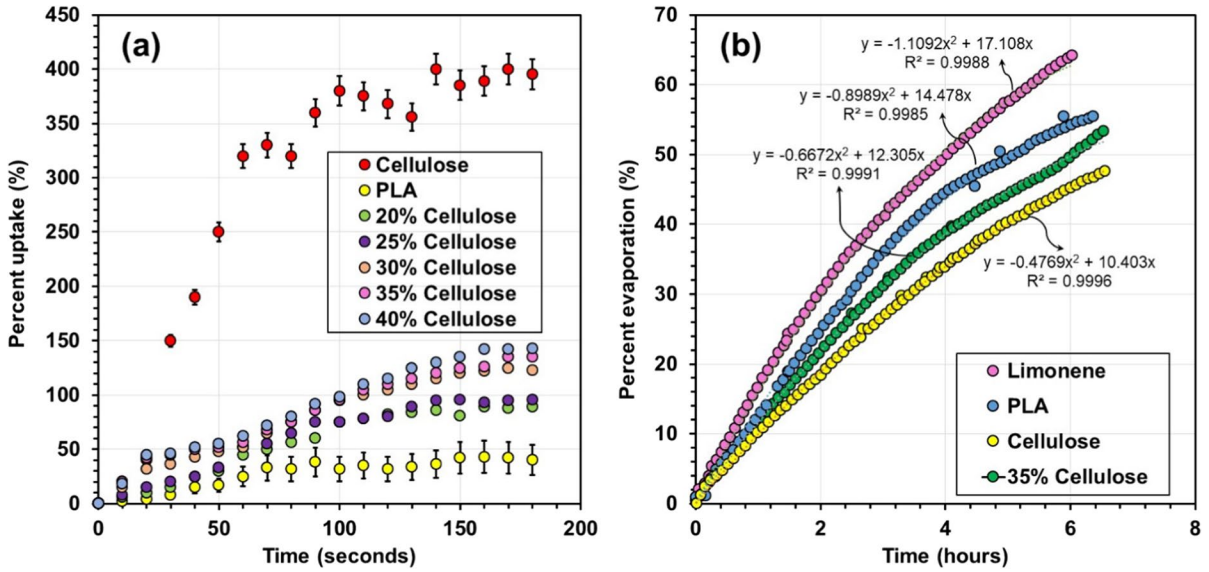

Fig. 5 **a** Limonene uptake due to 3 min. immersion experiments and **b** Percent evaporation of limonene from pure PLA, cellulose tissue and from the composite containing 35 wt% cellulose at 30 °C and 15% RH conditions

In Fig. 4 the surface and cross section SEM micrographs of 40 wt. % and 20wt% PLA/cellulose composites are displayed. The density of the exposed fibers on the surface increase as the weight percent of cellulose in the films increase as seen in Fig. 4a, b. Cross section images in Fig. 4c, d show a good degree of penetration of the cellulose fibers into the PLA film during hot pressing process.

Limonene is a colorless liquid aliphatic hydrocarbon categorized as a cyclic monoterpene, and is the major component in the oil of citrus fruit peels. It is a natural essential oil and as such, cellulose fibers are expected to absorb limonene. In fact, wood-derived cellulosic fibers were shown to absorb heavier oils such as simulated crude oil, demonstrating their possible use as absorbents in the case of oil spills (Moreno et al. 2020). Dry Kraft cellulose fibers demonstrated a sorption capacity of about six parts of oil per unit mass of fiber. Depending on the fiber source like hard and soft, and bleaching conditions, the oil uptake values could change (Moreno et al. 2020; Zhou et al. 2001). Cellulose micro and nanofibers are excellent natural matrices for essential oil uptake and release for various functional applications including food packaging (Payne et al. 2012; Hubbe et al. 2013). Figure 5 shows limonene uptake (Fig. 5a) and evaporation (boiling point of limonene is 176 °C) rates from dry cellulose tissues, pure PLA and various PLA-fiber composites. The cellulosic tissue could uptake limonene up to 4 times its weight after 100 s of immersion in a limonene bath. Conversely, pure PLA film uptakes much less limonene up to about 40% of its weight after 150 s of immersion. As shown in Fig. 5a, limonene uptake increases as the cellulose fiber concertation in the composites increases and a maximum of 150% uptake by weight was possible with 40 wt. % cellulose/PLA composites. This trend remained practically stable for composites between 30 and 40 wt. % cellulose as shown in Fig. 5a.

As mentioned before, limonene is a volatile essential oil and its evaporation rate is important in various applications such as antibacterial effect and flavoring in food (Zhang et al. 2020; Shen et al. 2014). At 30 °C and 15% RH, about 65% of pure limonene evaporates away within 6 h as shown in Fig. 5b. Limonene evaporation from PLA is somewhat hindered by the polymer matrix but about 55% limonene is lost from PLA within 6 h under the same conditions. The evaporation rate from cellulose fiber surfaces was slower and

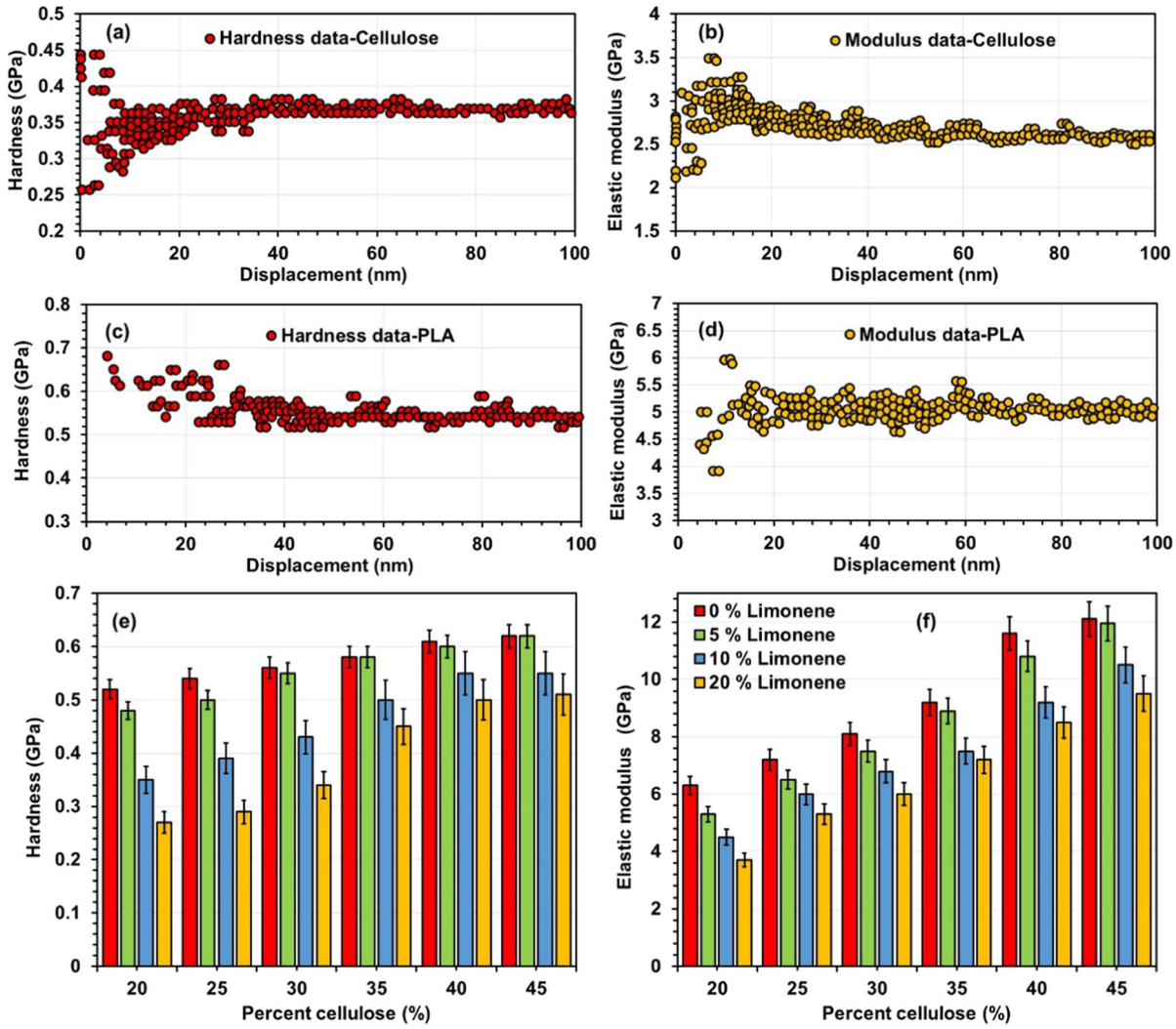

Fig. 6 AFM based indentation measurements. **a** Hardness versus displacement and **b** elastic modulus versus displacement data for cellulose fibers. **c** Hardness versus displacement and **d** elastic modulus versus displacement data for pure PLA film. **d** Average hardness as a function of limonene content for all the cellulose fiber-PLA composites. **e** Elastic moduli as a function of limonene content for all the cellulose fiber-PLA composites studied

was about 46% after 6 h. The evaporation rate from PLA-cellulose composites were within the 46–55% range as shown in Fig. 5b. All evaporation rates could be represented by a second order polynomial and, for example, for 35 wt% PLA/cellulose composite, the maximum loss of limonene occurred after 10 h under this specific conditions at 56 wt% . After this period, limonene loss declined significantly. Hence, considering the data in Fig. 5, one can argue that a 30 wt. % cellulose-PLA composite that had absorbed 50 wt% limonene will still function demonstrating antioxidant activity even after 10 h with about 25 wt% limonene content and after 24 h it will contain 20 wt% limonene if left uncovered in air at 30 °C and 15% RH. Evaporation of limonene from oil-in-water food emulsions also followed a similar trend and was shown to be sensitive to the ambient humidity and the limonene concentration in the oil phase of the emulsions could be modeled with a second order

polynomial during the initial evaporation phase and after several hours showed a linear dependence on time (Friberg 2007).

Thermomechanical properties of the PLA/cellulose fiber composites

In the following, we measured the mechanical properties of the fibers making up the tissue used in this work. Using nano-indentation detailed mechanical characterization of single fibers is possible. This method allows hardness testing at very small scale, and enables the measurement of the elastic (Young's) modulus and the hardness at a spatial resolution in the range of 10 to several 100 nm. The detailed characterization of cellulose fibers with this method is beyond the scope of this work, however, several published studies can be consulted for further insight into the effect of cellulose type, chemistry, treatment, regeneration and crystallinity, etc. on the fiber mechanical properties (Ganser et al. 2014; Lewczyk et al. 2020; Mohit et al. 2018; Gindl et al. 2006). Figure 6 shows hardness and elastic moduli of single cellulose fibers isolated from the tissue and pure PLA polymer, along with the PLA/cellulose fiber composites containing limonene. The hardness values of the Kraft cellulose fiber stabilized after an indentation depth of 30 nm and the average value was around 350 MPa (Fig. 6a). Similarly, the elastic modulus was

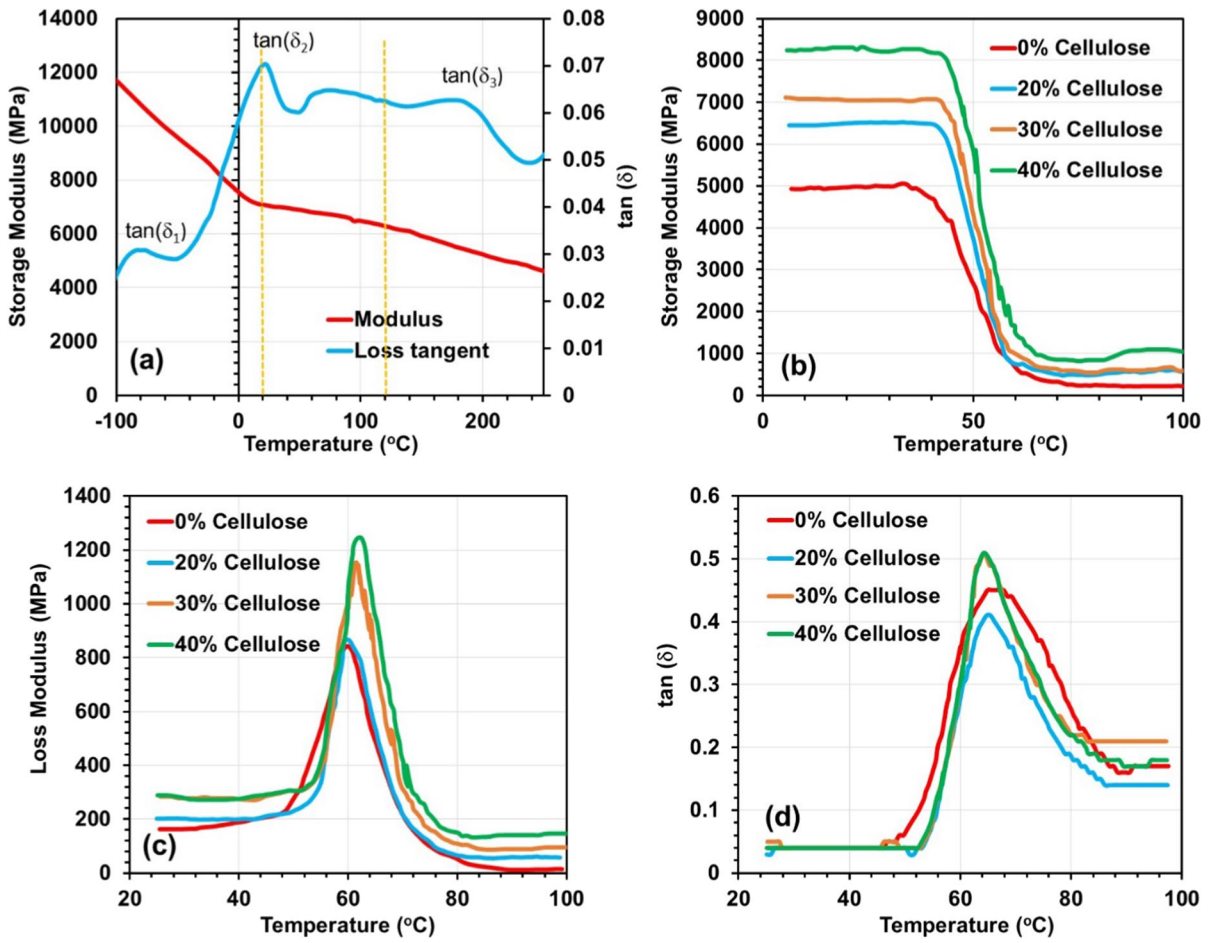

Fig. 7 Temperature dependent DMA measurements. **a** Changes in storage modulus and loss tangent (damping) of the tissue paper. **b** Changes in the storage modulus (the elastic character of a polymer/composite) for pure PLA and selected composites. Changes in the loss modulus (viscous behavior) **c** and loss tangent **d** of pure PLA (0% cellulose) and select composites

stable at an average value of 2.5 GPa after this indentation depth (Fig. 6b).

A detailed study by nano-indentation on the effect of thermo-mechanical cycles (recycling) on the physico-chemical properties of PLA (Adusumalli et al. 2010) indicated that PLA hardness remains stable at around 300 MPa and the elastic modulus at around 4.4 GPa, both of which appear to be in good agreement with the data reported herein. The hardness of the composites increased from 550 MPa to about 630 MPa as the cellulose fiber concentration of the composites increased (Fig. 6c, d), however, limonene reduced the hardness values by about 50% in composites containing cellulose up to 30 wt% , as seen in Fig. 6e.

These measurements appear to be in agreement with some recent studies in which cellulose microfibers were shown to increase the hardness of thermoplastics such as polyethylene by 100% at concentrations of about 40–45 wt% (Das et al. 2009). The effect of limonene on the hardness of the composites was less in PLA/cellulose fiber composites with 35 and 45 wt% cellulose. The elastic modulus of the composites increased as well with increasing cellulose inclusions (Fig. 5f). Similarly, based on other polymer-cellulose fiber composite studies (Das et al. 2009), the elastic moduli could be increased by three times at fiber loadings around 40-45wt. %. In this case, limonene also reduced the elastic moduli of the composites and the reduction was more pronounced for composites containing less than 35 wt. % cellulose. Limonene is a well-known plasticizer for pure PLA but also for PLA-nanocellulose composites (Fortunati et al. 2014; Pillin et al. 2008; Zhang et al. 2021), which reduces the elastic modulus of pure PLA and/or PLA/nanocellulose composites by two to three times depending on the nanocellulose loading. For instance, 3 wt. % nanocellulose reinforced PLA composites containing 20 wt% limonene had less than ½ elastic modulus of the composites with no limonene (Fortunati et al. 2014). A similar effect is obvious in Fig. 5f for composites with 20 and 25 wt% cellulose fiber reinforced PLA composites with 20wt% limonene.

The temperature dependent viscoelastic properties of the tissue paper measured in N_2 gas is given in Fig. 7a. Note that the storage modulus describes the ability of a sample to store energy and reflects the stiffness of paper samples and the loss tangent indicates damping behavior. Certain zones are visible in the storage moduli curves of the paper samples in Fig. 7a. For various types of Kraft papers, these zones were classified into four regions over a temperature range of − 50 to 200 °C as: vitreous state (below − 20 °C), devitrification (up to 25 °C), plateau (25–75 °C) and bond disruption (above 75 °C) (Siddiqui et al. 2021). In this case, we identify three clear zones in the range of − 120 to 270 °C. The tissue paper tested in nitrogen exhibited loss tangent peaks corresponding to temperatures of − 87 °C (tan δ_1) that is associated with the motion of segments of intra/inter molecular hydrogen bonding in cellulose.

Another one at 23 °C (tan δ_2) that is associated with the motion of a non-cellulosic material-cellulose interactions and the third one at186°C (tan δ_3), which is associated with the motion of segments in an amorphous region. The stabilization of tan δ (relatively constant state) between 70 and 150 °C is generally related to the pulp source (soft or hard wood) properties and fiber–fiber bonding strength. Moreover, this zone also reflects the production history of the paper sheet such as the wet pressing during sheet making that can tune tensile strength and stretch value of papers (Arrieta et al. 2014; Walker 2001). The tan δ measurements reported for similar bleached softwood pulp determined by using a non-intrusive Brillouin Light Scattering (BLS) micro-spectroscopy produced similar results in agreement with the measurement in Fig. 7a (Seth 2004).

The temperature dependence of the storage modulus, loss modulus and tan δ of pure PLA and selected PLA/cellulose fiber composites are shown in Fig. 7b in which the cellulose fiber inclusion increased the storage modulus for all the composites particularly at temperatures below 50 °C. This can be attributed to the stiffness characteristic of the reinforcement that allows greater degree of stress transfer at the interface (Ververis et al. 2007). Composites with 20 wt% cellulose induced more than 1.0 GPa enhancement in storage modulus. A similar effect was also measured between the composites with 30 and 40 wt. % cellulose fiber loadings. A significant decrease in the storage modulus was measured between 50 and 70 °C, which also corresponds to the glass transition region. The reduction in storage modulus as a function of temperature is correlated with the decrease in the polymer viscosity and the subsequent increase in polymer chain mobility (Elsayad et al. 2020). It was

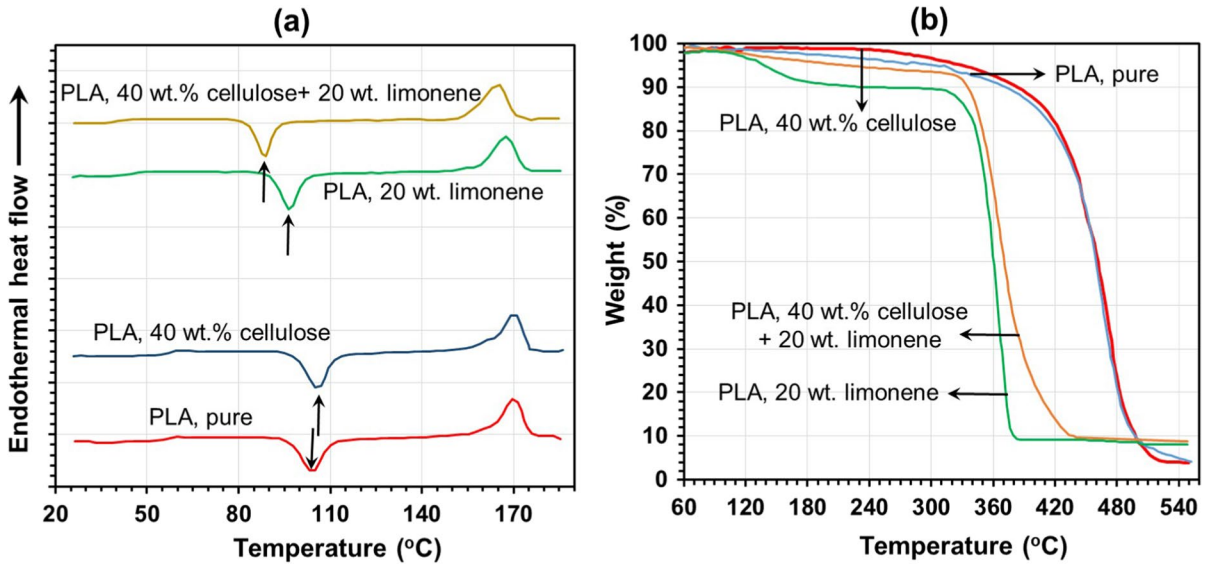

Fig. 8 **a** DSC thermograms of pure PLA and selected cellulose/PLA/limonene composites. Arrows show cold crystallization temperatures. **b** Thermogravimetric analysis (TGA) curves for pure PLA and selected cellulose/PLA/limonene composites

Table 2 Glass transition temperature (T_g), cold crystallization temperature (T_{cc}), melting temperature (T_m), crystallization enthalpy (ΔH_{cc}) and degree of crystallinity (X_{cc}) as well as enthalpy of melting (ΔH_m) data of the selected samples extracted from the DSC thermograms

Samples	Sample number	T_g (°C)	T_{cc} (°C)	ΔH_{cc} (J/g)	X_{cc} (%)	T_m (°C)	ΔH_m (J/g)
PLA (Control)	1	56.9	103.6	6.4	6.8	169.0	15.2
PLA-limonene (20 wt%)	2	47.1	96.2	29.2	34.7	166.4	35.5
PLA-cellulose (40 wt%)	3	61.0	105.2	34.0	37.8	169.1	38.5
PLA-cellulose-limonene*	4	42.7	88.7	25.2	31.3	164.1	36.3

* Sample 4 is PLA-40 wt% cellulose plasticized with 20 wt% limonene

reported that in PLA composites reinforced with cellulose fibers exceeding 50 wt% cellulose concentrations, at temperatures above 70–80 °C, the composites can demonstrate much less decrease in modulus due to the restriction in chain mobility of the matrix with stiffer cellulose fibers (Elsayad et al. 2020). Figure 7c displays the loss moduli of pure PLA and the selected composites and the glass transition temperature (T_g) occurs at the peak of each measured curve. The T_g values of the composites with 30 and 40 wt% cellulose fiber concentrations are slightly higher (~63 °C) than pure PLA and PLA with 20 wt% cellulose fibers (~59 °C). The increase in T_g is generally ascribed to the segmental immobilization of polymer matrix chains at the filler surface in which the rough surface topography of the cellulose might contribute to a good mechanical interlocking between the cellulose and the polymer (Bledzki et al. 2009). The ratio of the loss modulus to storage modulus is the tan δ or the damping factor. The variation of the tan δ as a function of temperature is shown in Fig. 7d. The damping or the tan δ is a measure of how efficient a material loses energy to molecular rearrangements and internal friction. The damping peak of 20 wt. % cellulose fiber composite displayed a decrease in magnitude compared with pure PLA. This can be attributed to the decrease in the mobility of the polymer chains on the addition of the fibers. This trend suggests that fibers and the PLA matrix have a strong interfacial adhesion. However, the tan δ was found to increase in

the 30 and 40 wt. % cellulose fiber composites. This suggests existence of higher damping at the interfaces and poorer interfacial bonding between the polymer and the fiber occurs at higher concentrations (Huda et al. 2006). This effect can be tuned if more elastic fibers are used or fiber surfaces are chemically modified. In fact, 20 wt% limonene containing PLA/cellulose fiber composites (30 wt. % cellulose) displayed (not shown here for brevity) lower damping energy as limonene plasticized both polymers (Mohanty et al. 2006; Pothan et al. 2003); but the slow evaporation of the essential oil reverses this measurement over time (Fortunati et al. 2014).

DSC thermograms of some selected samples such as pure PLA, PLA with 40 wt% cellulose and PLA and PLA/cellulose plasticized with limonene are shown in Fig. 8a. Thermal parameters with respect to glass transition temperature (T_g), cold crystallization temperature (T_{cc}), melting temperature (T_m), crystallization enthalpy (ΔH_{cc}) and degree of crystallinity (X_{cc}) are tabulated in Table 2. With regards to the non-plasticized composites, Tg increases slightly from 56.9 °C (pure PLA) to 60.9 °C (40 wt% cellulose fibers). This is consistent with previous research findings on the use of kenaf, bamboo and cotton to reinforce polymers, which can be due to the impeding of movement that the steric hindrance of cellulose fibers causes to PLA molecular chain (Eichers et al. 2022; Herrera et al. 2016). Notably, the crystallinity of PLA increased significantly from 6.8% to 37.7% with the addition of 40 wt. % cellulose pulp fibers. This can be attributed to the enhanced nucleation near cellulose fibers. With regard to composites with limonene, the T_g, T_{cc}, and T_m of the PLA composites all decreased. This is attributed to the plasticizing effect of limonene that lowers the T_g in particular. Similar findings have been reported by plasticization studies such as ATBC, plant oil, PEG, whereby the addition of plasticizer decreased the T_g of both pure PLA and the PLA composites. The plasticizers increase the segmental mobility of PLA chains and enhance the amorphous plastic deformation. Therefore, the decreased T_g is also assumed to decrease the tensile strength and increase the elongation at break.

Figure 8b shows the TGA curves of the same materials. Pure PLA and PLA with 40 wt. % cellulose feature similar weight loss trend with slight

Table 3 Percent water uptake and WVP data for the samples tested

Samples	Sample number	Water uptake (%)	WVP ($kgmm^{-2}\ s^{-/1}\ Pa^{-1}$)
PLA (Control)	1	6.8	2.31
PLA-limonene (20 wt%)	2	3.8	1.93
PLA-cellulose (40 wt%)	3	8.1	0.93
PLA-cellulose-limonene*	4	3.6	0.73

* Sample 4 is PLA-40 wt.% cellulose plasticized with 20 wt.% limonene

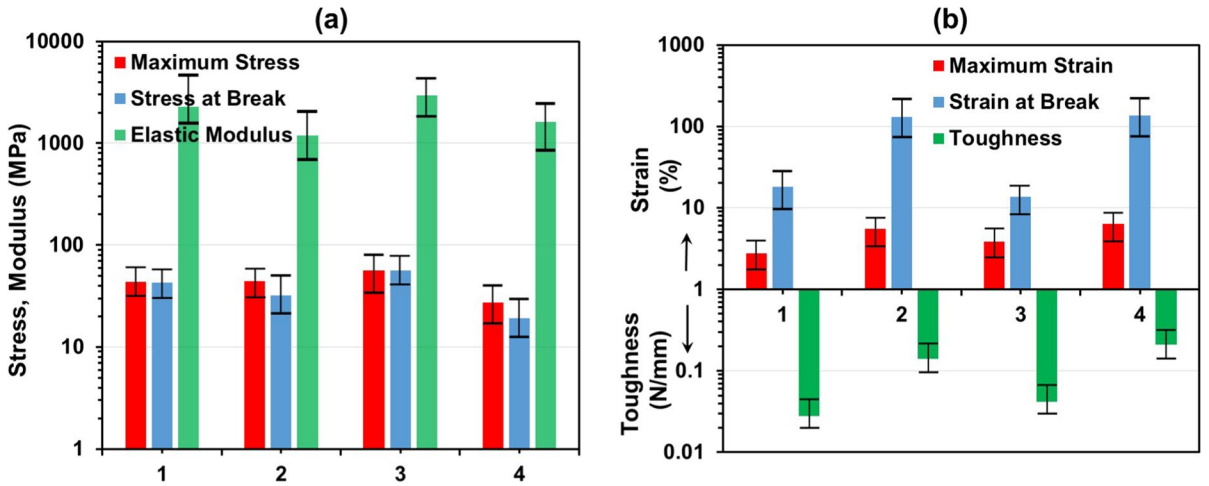

Fig. 9 **a** Mechanical properties (stress and moduli) of selected samples identified in Table 2, and **b** strain and toughness values of the samples

increase in the onset degradation temperature in the case of the PLA-cellulose composite. The pure PLA exhibited an onset temperature of 341.9 °C and a degradation temperature of 380.7 °C, which increased to 352.3, and 392.7 °C, respectively; once cellulose fibers were incorporated into the PLA matrix. Presence of limonene in both polymeric systems significantly shifted the degradation curves to 296.5 °C and 323.7 °C for PLA/limonene composite and PLA/cellulose/limonene composite, respectively.

Finally, the tensile properties of the selected composites listed in Table 2 are shown in Fig. 9. Figure 9a shows that the elastic (Young's) modulus of PLA increases by about 700 MPa when compounded with cellulose fibers. Also, when PLA is plasticized with 20 wt% limonene, The elastic modulus declines from 2260 to 1186 MPa. In the case of limonene plasticized PLA-cellulose composite, the elastic modulus improves to 1623 MPa with a strain at break value of about 130% which is similar to limonene plasticized pure PLA. Moreover, the toughness of the PLA-cellulose films plasticized with limonene is as high as PLA-cellulose composites that is around 0.6 N/mm (Fig. 9b). This value is practically a measure of the ability of a polymeric film to absorb energy (at the strain rate of the test instrument), and designates the durability of the film when subjected to either a repetitive or dynamic stressing or straining. Tensile energy absorption expresses the "toughness" of the film. Plasticized composites films feature better toughness value than the neat PLA film tested in this study. Based on these detailed mechanical property characterization results, it can be concluded that the materials developed in this study are comparable with other PLA-cellulose fiber composites as well as PLA-cellulose nanofiber (CNF) composites that were developed primarily for general food packaging applications (Mokhena et al. 2018; Khosravi et al. 2020).

Finally, the water uptake and water vapor permeation (WVP) values of pure PLA and the composites displayed in Fig. 9 are shown in Table 3. Clearly, the water uptake of pure PLA was high, about up to $6.8 \pm 0.08\%$ after immersing in water and saturation. The water uptake of limonene plasticized PLA (sample 2) significantly decreased to $3.8 \pm 0.02\%$ (Table 3), which was caused by the strong plasticizer–matrix interfacial interaction and the hydrophobicity of limonene. The water uptake of the cellulose/PLA composite (sample 3) was about $8.1 \pm 0.03\%$, higher compared to pure PLA due to the presence of the cellulose fibers. Plasticizing this composite with limonene (sample 4 in Table 2) reduced the water uptake to $3.6 \pm 0.04\%$ levels that can be quite adaptable for packaging applications. Similarly, WVP followed a similar trend where sample 4 had less than half WVP compared to pure PLA.

Antioxidant activity of the composites

D-limonene is a monocyclic terpene that is consumed by humans largely as an ingredient of traditional food such as citrus fruits, carrots, coffee, orange and nutmeg (Roberto et al. 2010). Moreover, D-limonene is generally recognized as a safe flavoring agent that can be found in common food items such as fruit juices, soft drinks, baked goods, ice cream and puddings. In previous studies, it was shown that monoterpenes like limonene possess antioxidant activity on DPPH models (Junior et al. 2009). It is also a potent anticancer and anti-tumor growth agent (Elson et al. 1988). A very recent work revealed that limonene can be very effective against Alzheimer's disease (Piccialli et al. 2021). In this work, we measured the antioxidant activity of limonene infused PLA-cellulose fiber composites with three different assays to ensure and confirm the functionality of the composites. Figure 10 shows both short term (~2-h) and long-term (3 days) antioxidant activity of the selected composites. As control samples, we measured the antioxidant activity of pure limonene and the PLA film containing 20 wt% limonene. In Fig. 10a, the DPPH antioxidant assay results are displayed. PLA film containing 20 wt% limonene quickly reaches an antioxidant level of 80% within ½ hour, which follows approximately the trend measured for pure limonene. Afterwards, the effect remains constant and does not change until the radicals start to degrade in solution (not shown here for brevity); hence, no long-term measurements were shown.

The 20 wt% cellulose fiber PLA composite follows a similar trend to PLA in the first 20 min but afterwards the effect slows down possibly due to diffusion of limonene from the cellulose fibers to the polymer surface and after to the solution. Once the 80 min marker was reached, the radical scavenging activity accelerates and reaches roughly to 70%. The

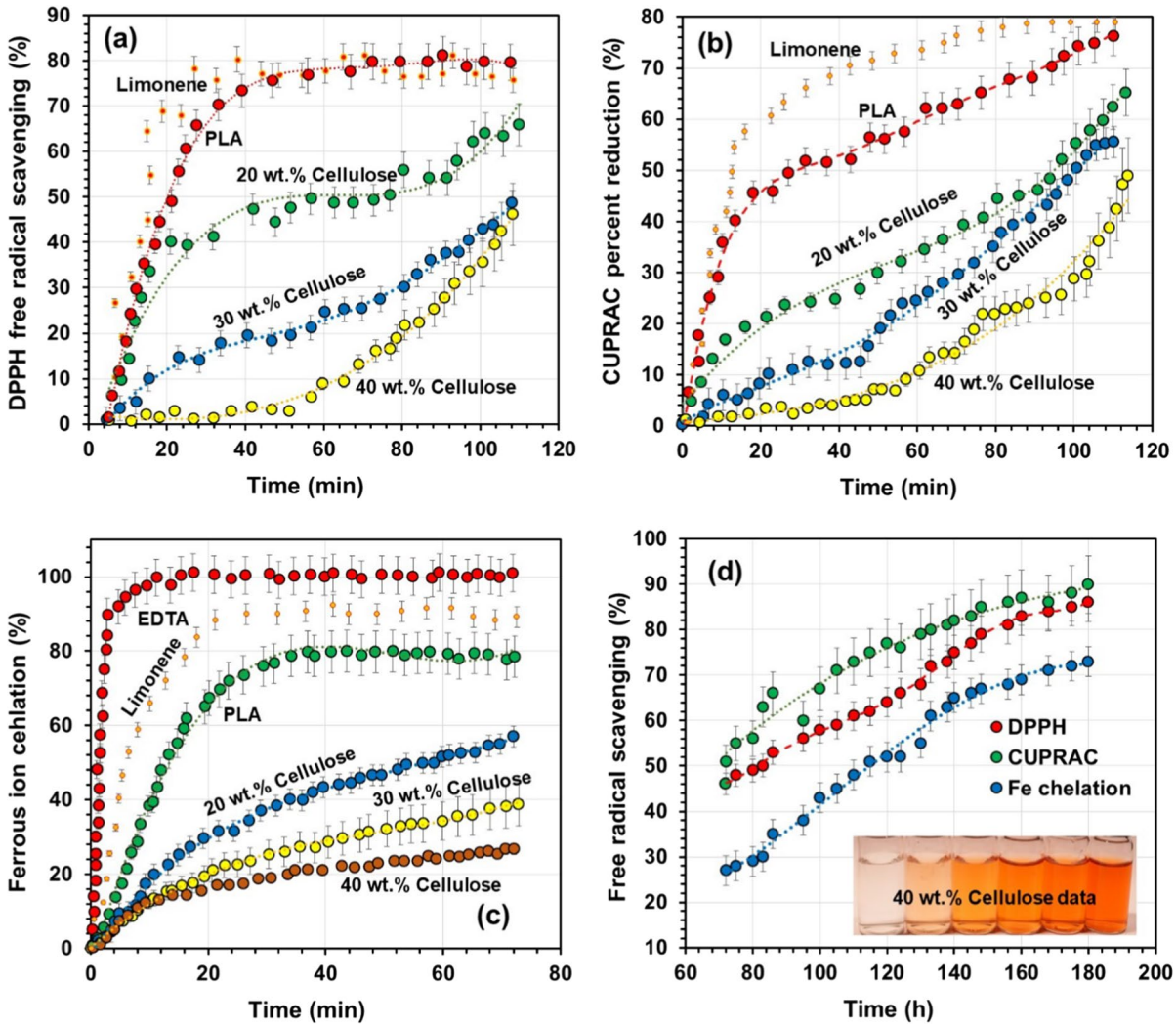

Fig. 10 **a** DDPH free radical scavenging assay measurements for short time (3 h) from selected samples including pure limonene as control. **b** Short term (3 h) CUPRAC percent ion reduction measurements from selected samples including limonene as control. **c** Percent ferrous ion chelation experiments (3-h period) for selected samples including EDTA and limonene as control. **d** Long term sustained release and free radical scavenging (all assays) activity of 40 wt% cellulose fiber PLA composite. The inset shows photographs of the color changes during the CUPRAC assay

30 wt% cellulose fiber/PLA composite shows a slow diffusion controlled antioxidant activity due to more embedded cellulose fibers in the PLA matrix and at the end of 100 min, 50% scavenging activity could be measured. In the case of 40 wt% cellulose fiber/PLA composites, very little radical scavenging activity occurs in the first hour, however, a steady increase occurs afterwards up to 50% level.

This indicates that most of the limonene infused within the cellulose fibers that are embedded in the PLA matrix experience a diffusional resistance that was gradually overcome after 60 min. The main migration activities of antioxidants include diffusion in the polymer structure, transfer from the bulk to the surface and distribution between interfaces. In the case of polymer composites, the interfacial diffusion between the polymers (i.e., cellulose fiber-PLA) can take longer than bulk diffusion (Kuai et al. 2021; Jamshidian et al. 2013) particularly if the interface concentrations (i.e., filler concentrations) are high.

A recent study evaluated the CUPRAC antioxidant activity of R-(+)-limonene that was extracted from

orange waste by the process of solid-state fermentation (Bier et al. 2019). Therein, the authors demonstrated that the extracted R-(+)-limonene and other terpene rich components had promising antioxidant effect in terms of Trolox equivalent scale but not as high as common polyphenols (Özyürek et al. 2011). In the present case, both pure limonene and limonene released from PLA films demonstrated about 80% cupric ion reducing capacity after about 1½ hour, as seen in Fig. 10b. The cupric (Cu^{+2}) reducing capacity of the PLA-cellulose fiber composites were somewhat different from the trend demonstrated in the DPPH scavenging dynamics of Fig. 10a. For instance, the 20 wt% cellulose fiber composite had much more sluggish cupric reduction rate within the first half hour compared to scavenging performance in Fig. 10a. This may be related to the fact that CUPRAC method is sensitive to the hydrophilicity and lipophilicity of the antioxidant molecules and the solvent medium. Çelik et al. (2010) established that in the presence of CUPRAC test reagents in solvent, lipophilic antioxidants can demonstrate various possible polymerization, depolymerization, and H-bonding interactions either with the polymer matrix or among themselves and with solvent molecules. This can reduce or interfere with the electron-transfer capability and reflects as changes in the reduction dynamics during measurements, which may be the case in the first half hour of the test conditions for PLA-cellulose fiber composites. However, at the end of about 1½ hour measurement, the final antioxidant percentage capability of all the samples were similar to the DPPH radical scavenging performance. Hence, limonene is able to diffuse out from the composites into the medium regardless of the antioxidant assay tested.

Figure 10c shows the ferrous (Fe^{2+}) metal ion chelation activity of the composites. Earlier studies have demonstrated that many plant terpenoids are strong endogenous metal chelating agents. In fact, many terpenoids with 40 µg/ml concentration demonstrated about 55% chelation of ferrous ions (Mohandas and Kumaraswamy 2018). Ethylenediaminetetraacetic acid (EDTA) is a strong metal binding agent and it shows a very robust ferrous ion chelation activity as shown in Fig. 10c. Within the first 10 min, EDTA showed 100% chelating effect, whereas pure limonene demonstrated about 87% chelating activity after 20 min and did not improve any further. Limonene released from pure PLA and the PLA-cellulose fiber composites also demonstrated ferrous ion chelating activity. Pure PLA film chelating activity gradually increased to about 80% within the first 40 min whereas the PLA-cellulose fiber composites displayed much slower effects and the 40 wt% cellulose composite could only reach 27% activity after about 70 min. The effect from the 40 wt. % cellulose composite appears to be comparable to the iron chelating activity of limonene present in wines (Di Sotto et al. 2013). Therein, limonene demonstrated the lowest effect (about 25%) compared to other terpinols of wine such as α-terpineol (100%) and 1,8-cineol (45%). However, as Fig. 10d shows that due to the gradual limonene release form the 40 wt% cellulose fiber composite, the antioxidant activity further increases and reaches to 70 and 80% levels depending on the antioxidant assay after 3 days of constant monitoring. This confirms that limonene is not strongly bound in the composites studied herein and shows sustained release dynamics. In general, encapsulated lipophilic antioxidants demonstrate sustained release activity that can be maintained for up to a few days (Chen et al. 2015; Biswick et al. 2010). If one considers active packaging made from these composites, correct and slow dosing of such natural antioxidants can sustain and prolong food quality and shelf life.

Conclusions

Limonene absorbed hygienic cellulose tissue fibers were impregnated into PL films hot pressing to produce antioxidant composites. Up to 40 wt% cellulose fibers could be impregnated into the PLA films while maintaining good mechanical properties and flexibility. FTIR measurements on the composites indicated establishment of some hydrogen bonds between PLA and cellulose and weak p-hydrogen bonds between limonene and PLA. DMA measurements showed that tan δ increased in the 30 and 40 wt% cellulose fiber composites suggesting the existence of higher damping at the interfaces and poorer interfacial bonding between the polymer and the fiber occurs at higher concentrations. Limonene inclusion up to 20 wt% in these composites lowered the damping energy in the composites indicating effective plasticization. The glass transition of the composites were also decreased by limonene by up to 20 °C. Three different antioxidant assays (DPPH, CUPRAC and Ferrous

ion chelation) were used to study the antioxidant properties of the limonene modified cellulose fiber PLA composites. Within approximately two hours up to 70% radical scavenging activity was recorded in with DPPH and CUPRAC assays whereas ferrous ion chelation activity was much slower with less than 60%, however all samples sustained their antioxidant effect for at least one week with ferrous ion chelation levels exceeding 70%. Depending on the cellulose content of the composites, sustained release and antioxidant activity exceeded 80% in the CUPRAC and DPPH assay tests. These composites could be produced in large scale through a hot roll-to-roll press process and can be potentially used in active and protective packaging of fruits and cosmetic products.

Acknowledgments The authors express their gratitude to Ankara University (Türkiye) for providing facility access to carry out this study.

Authors contribution All authors contributed to the study, conception and design. The study was conceived by ISB with initial validation experiments. GB and AS performed extensive experimental work and developed methodologies and all authors interpreted and analyzed the data. All authors read and approved the final manuscript.

Funding GB acknowledges financial support from DS Bio ve Nanoteknoloji A. Ş (Türkiye).

Data availability Not applicable.

Declarations

Conflict of interest The authors declare that they have no known competing financial interests or personal relationships that could have appeared to influence this study.

Ethics approval and consent to participate Not applicable.

Consent for publication Not applicable.

References

Adusumalli RB, Mook WM, Passas R, Schwaller P, Michler J (2010) Nanoindentation of single pulp fibre cell walls. J Mater Sci 45:2558–2563. https://doi.org/10.1007/s10853-010-4226-9

Apak R, Güçlü K, Demirata B, Özyürek M, Çelik SE, Özyurt D et al (2007) Comparative evaluation of various total antioxidant capacity assays applied to phenolic compounds with the CUPRAC assay. Molecules 12:1496–1547. https://doi.org/10.3390/12071496

Arrieta MP, López J, Ferrándiz S, Peltzer MA et al (2013) Characterization of PLA-limonene blends for food packaging applications. Polym Testing 32:760–768. https://doi.org/10.1016/j.polymertesting.2013.03.016

Arrieta MP, López J, Hernández A, Rayón E (2014) Ternary PLA–PHB–Limonene blends intended for biodegradable food packaging applications. Eur Polymer J 50:255–270. https://doi.org/10.1016/j.eurpolymj.2013.11.009

Asmatulu E, Twomey J, Overcash M (2014) Recycling of fiber-reinforced composites and direct structural composite recycling concept. J Compos Mater 48:593–608. https://doi.org/10.1177/0021998313476325

Assis TD, Reisinger LW, Pal L, Pawlak J, Jameel H, Gonzalez RW (2018) Understanding the effect of machine technology and cellulosic fibers on tissue properties–a review. BioResources 13:4593–4629. https://doi.org/10.15376/biores.13.2.DeAssis

Assis TD, Pawlak J, Jameel H, Reisinger LW, Kavalew D, Gonzalez RW (2020) Comparison between uncreped and creped handsheets on tissue paper properties using a creping simulator unit. Cellulose 27:5981–5999. https://doi.org/10.1007/s10570-020-03163-0

Aumnate C, Soatthiyanon N, Makmoon T, Potiyaraj P (2021) Polylactic acid/kenaf cellulose biocomposite filaments for melt extrusion based-3D printing. Cellulose 28:8509–8525. https://doi.org/10.1007/s10570-021-04069-1

Auras R, Harte B, Selke S (2006) Sorption of ethyl acetate and d-limonene in poly (lactide) polymers. J Sci Food Agric 86:648–656. https://doi.org/10.1002/jsfa.2391

Ayadi F, Bayer IS, Fragouli D, Liakos I, Cingolani R, Athanassiou A (2013) Mechanical reinforcement and water repellency induced to cellulose sheets by a polymer treatment. Cellulose 20:1501–1509. https://doi.org/10.1007/s10570-013-9900-z

Baltazar-y-Jimenez A, Sain M (2012) Effect of bismaleimide reactive extrusion on the crystallinity and mechanical performance of poly (lactic acid) green composites. J Appl Polym Sci 124:3013–3023. https://doi.org/10.1002/app.35331

Bayer G, Shayganpour A, Zia J, Bayer IS (2022) Polyvinyl alcohol-based films plasticized with an edible sweetened gel enriched with antioxidant carminic acid. J. Food Eng 323:111000. https://doi.org/10.1016/j.jfoodeng.2022.111000

Bier MCJ, Medeiros ABP, Kimpe ND, Soccol CR (2019) Evaluation of antioxidant activity of the fermented product from the biotransformation of R-(+)-limonene in solid-state fermentation of orange waste by Diaporthe sp. Biotechnol Res Innov 3:168–176. https://doi.org/10.1016/j.biori.2019.01.002

Biswick T, Park DH, Shul YG, Choy JH (2010) P-coumaric acid–zinc basic salt nanohybrid for controlled release and sustained antioxidant activity. J Phys Chem Solids 71:647–649. https://doi.org/10.1016/j.jpcs.2009.12.058

Bledzki AK, Jaszkiewicz A, Scherzer D (2009) Mechanical properties of PLA composites with man-made cellulose and abaca fibres. Compos Part A: Appl Sci Manuf 40:404–412. https://doi.org/10.1016/j.compositesa.2009.01.002

Brüster B, Adjoua YO, Dieden R, Grysan P, Federico CE, Berthé V, Addiego F (2019) Plasticization of polylactide with myrcene and limonene as bio-based plasticizers: conventional versus reactive extrusion. Polymers 11:1363–7894

Cao CX, Yuan J, Cheng JP, Han BH (2017) Synthesis of porous polymer/tissue paper hybrid membranes for switchable oil/water separation. Sci Rep 7:1–9. https://doi.org/10.1038/s41598-017-03265-z

Çelik SE, Özyürek M, Güçlü K, Apak R (2010) Solvent effects on the antioxidant capacity of lipophilic and hydrophilic antioxidants measured by CUPRAC, ABTS/persulphate and FRAP methods. Talanta 81:1300–1309. https://doi.org/10.1016/j.talanta.2010.02.025

Chen X, Zou LQ, Niu J, Liu W, Peng SF, Liu CM (2015) The stability, sustained release and cellular antioxidant activity of curcumin nanoliposomes. Molecules 20:14293–14311. https://doi.org/10.3390/molecules200814293

Ciriminna R, Rodriguez ML, Cara PD, Sanchez JAL, Pagliaro M (2014) Limonene: a versatile chemical of the bioeconomy. Chem Commun 50:15288–15296. https://doi.org/10.1039/C4CC06147K

Dapkūnienė K, Strazdienė E (2006) Influence of layer orientation upon textile systems tensile properties. part 2. Investigation of tensile energy and linearity. Mater Sci (medžiagotyra) 12:247–252

Das K, Ray D, Bandyopadhyay NR, Ghosh T, Mohanty AK, Misra M (2009) A study of the mechanical, thermal and morphological properties of microcrystalline cellulose particles prepared from cotton slivers using different acid concentrations. Cellulose 16:783–793. https://doi.org/10.1007/s10570-009-9280-6

Dasmohapatra S, Assis TD, Reisinger LW, Pawlak J, Jameel H, Pal L, Golzalez R (2018) Performance and sustainability vs. the shelf price of tissue paper kitchen towels. Bioresources 13:6868–6892. https://doi.org/10.15376/biores.13.3.6868-6892

Dislaire C, Seantier B, Muzy M, Grohens Y (2021) Mechanical and hygroscopic properties of molded pulp products using different wood-based cellulose fibers. Polymers 13:3225. https://doi.org/10.3390/polym13193225

Du Y, Wu T, Yan N, Kortschot MT, Farnood R (2013) Pulp fiber-reinforced thermoset polymer composites: effects of the pulp fibers and polymer. Compos B Eng 48:10–17. https://doi.org/10.1016/j.compositesb.2012.12.003

Du Y, Wu T, Yan N, Kortschot MT, Farnood R (2014) Fabrication and characterization of fully biodegradable natural fiber-reinforced poly (lactic acid) composites. Compos B Eng 56:717–723. https://doi.org/10.1016/j.compositesb.2013.09.012

Eichers M, Bajwa D, Shojaeiarani J, Bajwa S (2022) Biobased plasticizer and cellulose nanocrystals improve mechanical properties of polylactic acid composites. Ind Crops Prod 183:114981. https://doi.org/10.1016/j.indcrop.2022.114981

Elsayad K, Urstöger G, Czibula C, Teichert C, Gumulec J, Balvan J, Hirn U (2020) Mechanical Properties of cellulose fibers measured by Brillouin spectroscopy. Cellulose 27:4209–4220. https://doi.org/10.1007/s10570-020-03075-z

Elson CE, Maltzman TH, Boston JL, Tanner MA, Gould MN (1988) Anti-carcinogenic activity of d-limonene during the initiation and promotion/progression stages of DMBA-induced rat mammary carcinogenesis. Carcinogenesis 9:331–332. https://doi.org/10.1093/carcin/9.2.331

Fortunati E, Luzi F, Puglia D, Dominici F, Santulli C, Kenny JM, Torre L (2014) Investigation of thermo-mechanical, chemical and degradative properties of PLA-limonene films reinforced with cellulose nanocrystals extracted from Phormium tenax leaves. Eur Polym J 56:77–91. https://doi.org/10.1016/j.eurpolymj.2014.03.030f

Frank ES, Fan H, Shrestha M, Riahi S, Tobias DJ, Grassian VH (2020) Impact of adsorbed water on the interaction of limonene with hydroxylated SiO_2: implications of π-hydrogen bonding for surfaces in humid environments. J Phys Chem A 124:10592–10599. https://doi.org/10.1021/acs.jpca.0c08600

Friberg SE (2007) Evaporation from a limonene emulsion. J Dispersion Sci Technol 28:11–20. https://doi.org/10.1080/01932690600992241

Frone AN, Panaitescu DM, Chiulan I, Nicolae CA, Damian CM (2016) The effect of cellulose nanofibers on the crystallinity and nanostructure of poly (lactic acid) composites. J Mater Sci 51:9771–9791. https://doi.org/10.1007/s10853-016-0212-1

Ganser C, Hirn U, Rohm S, Schennach R, Teichert C (2014) AFM nanoindentation of pulp fibers and thin cellulose films at varying relative humidity. Holzforschung 68:53–60. https://doi.org/10.1515/hf-2013-0014

Gindl W, Konnerth J, Schöberl T (2006) Nanoindentation of regenerated cellulose fibres. Cellulose 13:1–7. https://doi.org/10.1007/s10570-005-9017-0

Graupner N, Herrmann AS, Müssig J (2009) Natural and man-made cellulose fibre-reinforced poly (lactic acid) (PLA) composites: an overview about mechanical characteristics and application areas. Compos A Appl Sci Manuf 40:810–821. https://doi.org/10.1016/j.compositesa.2009.04.003

Gurav SP, Bereznitski A, Heidweiller A, Kandachar PV (2003) Mechanical properties of paper-pulp packaging. Compos Sci Technol 63:1325–1334. https://doi.org/10.1016/S0266-3538(03)00104-0

Haque ANMA, Remadevi R, Naebe M (2018) Lemongrass (Cymbopogon): a review on its structure, properties, applications and recent developments. Cellulose 25:5455–5477. https://doi.org/10.1007/s10570-018-1965-2

Hebeish A, Fouda MM, Hamdy IA, Sawy SME, Mohdy FAA (2008) Preparation of durable insect repellent cotton fabric: limonene as insecticide. Carbohyd Polym 74:268–273. https://doi.org/10.1016/j.carbpol.2008.02.013

Herrera N, Salaberria AM, Mathew AP, Oksman K (2016) Plasticized polylactic acid nanocomposite films with cellulose and chitin nanocrystals prepared using extrusion and compression molding with two cooling rates: effects on mechanical, thermal and optical properties. Compos A Appl Sci Manuf 83:89–97. https://doi.org/10.1016/j.compositesa.2015.05.024

Hirn U, Schennach R (2015) Comprehensive analysis of individual pulp fiber bonds quantifies the mechanisms of fiber bonding in paper. Sci Rep 5:1–9. https://doi.org/10.1038/srep10503

Hubbe MA (2006) Bonding between cellulosic fibers in the absence and presence of dry-strength agents–a review. BioResources 1:281–318. https://doi.org/10.15376/biores.1.2.281-318

Hubbe MA (2014) Prospects for maintaining strength of paper and paperboard products while using less forest resources: a review. Bioresources 9:1634–1763

Hubbe MA, Venditti RA, Rojas OJ (2007) What happens to cellulosic fibers during papermaking and recycling? A review. Bioresources 2:739–788. https://doi.org/10.15376/BIORES.2.4.739-788

Hubbe MA, Rojas OJ, Fingas M, Gupta BS (2013) Cellulosic substrates for removal of pollutants from aqueous systems: a review. 3. Spilled oil and emulsified organic liquids. BioResources 8:3038–3097. https://doi.org/10.15376/biores.6.2.2161-2287

Huda MS, Drzal LT, Misra M, Mohanty AK (2006) Wood-fiber-reinforced poly (lactic acid) composites: evaluation of the physicomechanical and morphological properties. J Appl Polym Sci 102:4856–4869. https://doi.org/10.1002/app.24829

Ismail MY, Patanen M, Kauppinen S, Kosonen H, Hall SA, Liimatainen H (2020) Surface analysis of tissue paper using laser scanning confocal microscopy and micro-computed topography. Cellulose 27:8989–9003. https://doi.org/10.1007/s10570-020-03399-w

Jahangir ES, Olson JA (2020) Low consistency refined ligno-cellulose microfibre: an MFC alternative for high bulk, tear and tensile mechanical pulp papers. Cellulose 27:2803–2816. https://doi.org/10.1007/s10570-019-02956-2

Jamshidian M, Tehrany EA, Desobry S (2013) Antioxidants release from solvent-cast PLA film: investigation of PLA antioxidant-active packaging. Food Bioprocess Technol 6:1450–1463. https://doi.org/10.1007/s11947-012-0830-9

Junior MRM, Silva TAR, Franchi GC, Nowill A, Pastore GM, Hyslop S (2009) Antioxidant potential of aroma compounds obtained by limonene biotransformation of orange essential oil. Food Chem 116:8–12. https://doi.org/10.1016/j.foodchem.2009.01.084

Kawabata S, Niwa M, Yamashita Y (2002) Recent developments in the evaluation technology of fiber and textiles: toward the engineered design of textile performance. J Appl Polym Sci 83:687–702. https://doi.org/10.1002/app.2264

Khalil HA, Tye YY, Chow ST, Saurabh CK, Paridah MT, Dungani R, Syakir MI (2017) Cellulosic pulp fiber as reinforcement materials in seaweed-based film. Bioresources 12:29–42. https://doi.org/10.15376/biores.12.1.29-42

Khosravi A, Fereidoon A, Khorasani MM, Naderi G, Ganjali MR, Zarrintaj P, Gutiérrez TJ (2020) Soft and hard sections from cellulose-reinforced poly (lactic acid)-based food packaging films: a critical review. Food Packag Shelf Life 23:100429. https://doi.org/10.1016/j.fpsl.2019.100429

Kojima Y, Kawabata A, Kobori H, Suzuki S, Ito H, Makise R, Okamoto M (2016) Reinforcement of fiberboard containing lingo-cellulose nanofiber made from wood fibers. J Wood Sci 62:518–525. https://doi.org/10.1007/s10086-016-1582-3

Kouko J, Turpeinen T, Kulachenko A, Hirn U, Retulainen E (2020) Understanding extensibility of paper: role of fiber elongation and fiber bonding. Tappi J 19:125–135. https://doi.org/10.32964/TJ19.3.125

Kuai L, Liu F, Chiou BS, Avena-Bustillos RJ, McHugh TH, Zhong F (2021) Controlled release of antioxidants from active food packaging: a review. Food Hydrocoll 120:106992. https://doi.org/10.1016/j.foodhyd.2021.106992

Lam YL, Kan CW, Yuen CWM, Au CH (2011) Fabric objective measurement of the plasma-treated cotton fabric subjected to wrinkle-resistant finishing with BTCA and TiO_2 system. Fibers Polym 12:626–634. https://doi.org/10.1007/s12221-011-0626-y

Lee J, Koo N, Min DB (2006) Reactive oxygen species, aging and antioxidative nutraceuticals Compr. Rev Food Sci Food Saf 1:21–33. https://doi.org/10.1111/j.1541-4337.2004.tb00058.x

Leppänen I, Vikman M, Harlin A, Orelma H (2020) Enzymatic degradation and pilot-scale composting of cellulose-based films with different chemical structures. J Polym Environ 28:458–470. https://doi.org/10.1007/s10924-019-01621-w

Lewczyk DC, Cohan JW, Goetz ML, Trafford BL, Fuller RL, Sparks JR (2020) Kinetic treatment of evaporation via thermogravimetric analysis: the case of d-Limonene. Ind Eng Chem Res 59:15069–15074. https://doi.org/10.1021/acs.iecr.0c02864

Liu S, Li X, Chen L, Li L, Li B, Zhu J (2018) Tunable d-limonene permeability in starch-based nanocomposite films reinforced by cellulose nanocrystals. J Agric Food Chem 66:979–987. https://doi.org/10.1021/acs.jafc.7b05457

Lopes S, Afonso C, Fernandes I, Barreiro MF, Costa P, Rodrigues AE (2019) Chitosan-cellulose particles as delivery vehicles for limonene fragrance. Ind Crops Prod 139:111407. https://doi.org/10.1016/j.indcrop.2019.05.057

Maraveas C, Bayer IS, Bartzanas T (2021) Recent advances in antioxidant polymers: from sustainable and natural monomers to synthesis and applications. Polymers 13:2465. https://doi.org/10.3390/polym13152465

Mohandas GG, Kumaraswamy M (2018) Antioxidant activities of terpenoids from Thuidium tamariscellum (C. Muell.) Bosch. and Sande-Lac. a Moss. Pharmacogn J 10:645–649. https://doi.org/10.5530/pj.2018.4.106

Mohanty S, Verma SK, Nayak SK (2006) Dynamic mechanical and thermal properties of MAPE treated jute/HDPE composites. Compos Sci Technol 66:538–547. https://doi.org/10.5530/pj.2018.4.106

Mohit H, Selvan VAM (2018) A comprehensive review on surface modification, structure interface and bonding mechanism of plant cellulose fiber reinforced polymer based composites. Compos Interfaces 25:629–667. https://doi.org/10.1080/09276440.2018.1444832

Mokhena TC, Sefadi JS, Sadiku ER, John MJ, Mochane MJ, Mtibe A (2018) Thermoplastic processing of PLA/cellulose nanomaterials composites. Polymers 10:1363. https://doi.org/10.3390/polym10121363

Molina AIQ, Pasquale L, Debellis D, Tedeschi G, Athanassiou A, Bayer IS (2021) Responsive bio-composites from magnesium carbonate filled polycaprolactone and curcumin-functionalized cellulose fibers. Adv Sustain Syst 5:2100128. https://doi.org/10.1002/adsu.202100128

Montoille L, Vicencio CM, Fontalba D, Ortiz JA, Serna VM, Peponi L, Zapata PA (2021) Study of the effect of the addition of plasticizers on the physical properties of biodegradable films based on Kefiran for potential application as food packaging. Food Chem 360:129966. https://doi.org/10.1016/j.foodchem.2021.129966

Moreno MF, Stinson CJ, Shepherd RG, Welsh ID, Altaner C, Crittenden DL (2020) Temperature-dependent blue shifting of O–H stretching frequencies in crystalline cellulose explained. J Phys Chem B 124:4924–4930. https://doi.org/10.1021/acs.jpcb.0c02793

Moriam K, Rissanen M, Sawada D, Altgen M, Johansson LS, Evtyugin DV, Sixta H (2021) Hydrophobization of the man-made cellulosic fibers by incorporating plant-derived hydrophobic compounds. ACS Sustain Chem Eng 9:4915–4925. https://doi.org/10.1021/acssuschemeng.1c00695

Oliver WC, Pharr GM (1992) An improved technique for determining hardness and elastic modulus using load and displacement sensing indentation experiments. J Mater Res 7:1564–1583. https://doi.org/10.1557/JMR.1992.1564

Özyürek M, Güçlü K, Apak R (2011) The main and modified CUPRAC methods of antioxidant measurement. TrAC, Trends Anal Chem 30:652–664. https://doi.org/10.1016/j.trac.2010.11.016

Parfitt M, Vickerman JC, Mitchell R, Carr CM, Ince N, Knight P (2003) Surface analysis of softened paper by time-of-flight secondary ion mass spectrometry (ToF-SIMS) and the Kawabata evaluation system. J Mater Sci 38:2171–2177. https://doi.org/10.1557/JMR.1992.1564

Pawlak JJ, Frazier R, Vera RE, Wang Y, Gonzalez R (2022) The softness of hygiene tissue. Bioresources 17:3509–3550. https://doi.org/10.15376/biores.17.2.Pawlak

Payne KC, Jackson CD, Aizpurua CE, Rojas OJ, Hubbe MA (2012) Oil spills abatement: factors affecting oil uptake by cellulosic fibers. Environ Sci Technol 46:7725–7730. https://doi.org/10.1021/es3015524

Peltola H, Immonen K, Johansson LS, Virkajärvi J, Sandquist D (2019) Influence of pulp bleaching and compatibilizer selection on performance of pulp fiber reinforced PLA biocomposites. J Appl Polym Sci 136:47955. https://doi.org/10.1002/app.47955

Petrucci R, Fortunati E, Puglia D, Luzi F, Kenny JM, Torre L (2018) Life cycle analysis of extruded films based on poly (lactic acid)/cellulose nanocrystal/limonene: a comparative study with ATBC plasticized PLA/OMMT systems. J Polym Environ 26:1891–1902. https://doi.org/10.1007/s10924-017-1085-3

Piccialli I, Tedeschi V, Caputo L, Amato G, Martino LM, Feo VD, Pannaccione A (2021) The Antioxidant Activity of Limonene Counteracts Neurotoxicity Triggered byAβ1-42 Oligomers in Primary Cortical Neurons. Antioxidants 10:937. https://doi.org/10.3390/antiox10060937

Pillin I, Montrelay N, Bourmaud A, Grohens Y (2008) Effect of thermo-mechanical cycles on the physico-chemical properties of poly (lactic acid). Polym Degrad Stab 93:321–328. https://doi.org/10.1016/j.polymdegradstab.2007.12.005

Pirralho M, Flores D, Sousa VB, Quilhó T, Knapic S, Pereira H (2014) Evaluation on paper making potential of nine Eucalyptus species based on wood anatomical features. Ind Crops Prod 54:327–334. https://doi.org/10.1016/j.indcrop.2014.01.040

Poletto M, Pistor V, Zeni M, Zattera AJ (2011) Crystalline properties and decomposition kinetics of cellulose fibers in wood pulp obtained by two pulping processes. Polym Degrad Stab 96:679–685. https://doi.org/10.1016/j.polymdegradstab.2010.12.007

Pothan LA, Oommen Z, Thomas S (2003) Dynamic mechanical analysis of banana fiber reinforced polyester composites. Compos Sci Technol 63:283–293. https://doi.org/10.1016/S0266-3538(02)00254-3

Raabe J, Fonseca ADS, Bufalino L, Ribeiro C, Martins MA, Marconcini JM, Tonoli GHD (2015) Biocomposite of cassava starch reinforced with cellulose pulp fibers modified with deposition of silica (SiO_2) nanoparticles. Journal of Nanomater. https://doi.org/10.1155/2015/493439

Rehan M, Wahed NAA, Farouk A, Zawahry MME (2018) Extraction of valuable compounds from orange peel waste for advanced functionalization of cellulosic surfaces. ACS Sustain Chem Eng 6:5911–5928. https://doi.org/10.1021/acssuschemeng.7b04302

Reitbauer J, Harrer F, Eckhart R, Bauer W (2021) Focus variation technology as a tool for tissue surface characterization. Cellulose 28:6813–6827. https://doi.org/10.1007/s10570-021-03953-0

Roberto D, Micucci P, Sebastian T, Graciela F, Anesini C (2010) Antioxidant activity of limonene on normal murine lymphocytes: relation to H_2O_2 modulation and cell proliferation. Basic Clin Pharmacol Toxicol 106:38–44. https://doi.org/10.1111/j.1742-7843.2009.00467.x

Rosdi MHHM, Ahad NA, Shahdan D (2022) Comparison on oil and water absorption ability of various natural fiber. J. Phys. Conf. Ser. 2169:012021

Saedi S, Garcia CV, Kim JT, Shin GH (2021) Physical and chemical modifications of cellulose fibers for food packaging applications. Cellulose 28:8877–8897. https://doi.org/10.1007/s10570-021-04086-0

Sdrobiş A, Darie RN, Totolin M, Cazacu G, Vasile C (2012) Low density polyethylene composites containing cellulose pulp fibers. Compos B Eng 43:1873–1880. https://doi.org/10.1016/j.compositesb.2012.01.064

Sepúlveda FA, Rivera F, Loyo C, Canales D, Serna VM, Benavente R, Zapata PA (2022) Poly (lactic acid)/D-limonene/ZnO bio-nanocomposites with antimicrobial properties. J Appl Polym Sci 139:51542. https://doi.org/10.1002/app.51542

Seth RS (2004) Understanding sheet extensibility. In Annual Meeting-Pulp and Paper Technical Association of Canada (Vol. 90, No. A, pp. 51–60). Pulp and Paper Technical Association of Canada; 1999.

Shen Z, Kamdem DP (2015) Antimicrobial activity of sugar beet lignocellulose films containing tung oil and cedarwood essential oil. Cellulose 22:2703–2715. https://doi.org/10.1007/s10570-015-0679-y

Shen J, Fatehi P, Ni Y (2014) Biopolymers for surface engineering of paper-based products. Cellulose 21:3145–3160. https://doi.org/10.1007/s10570-014-0380-6

Siddiqui MN, Redhwi HH, Tsagkalias I, Vouvoudi EC, Achilias DS (2021) Development of bio-composites with enhanced antioxidant activity based on poly (lactic acid) with thymol, carvacrol, limonene, or cinnamaldehyde for active food packaging. Polymers 13:3652. https://doi.org/10.3390/polym13213652

Singh AA, Genovese ME, Mancini G, Marini L, Athanassiou A (2020) Green processing route for polylactic acid–cellulose fiber biocomposites. ACS Sustain Chem Eng 8:4128–4136. https://doi.org/10.1021/acssuschemeng.9b06760

Sotto AD, Durazzi F, Sarpietro MG, Mazzanti G (2013) Antimutagenic and antioxidant activities of some bioflavours from wine. Food Chem Toxicol 60:141–146. https://doi.org/10.1016/j.fct.2013.07.042

Suryanegara L, Nakagaito AN, Yano H (2010) Thermo-mechanical properties of microfibrillated cellulose-reinforced partially crystallized PLA composites. Cellulose 17:771–778. https://doi.org/10.1007/s10570-010-9419-5

Venkatarajan S, Athijayamani A (2021) An overview on natural cellulose fiber reinforced polymer composites. Mater Today: Proc 37:3620–3624. https://doi.org/10.1016/j.matpr.2020.09.773

Ververis C, Georghiou K, Danielidis D, Hatzinikolaou DG, Santas P, Santas R, Corleti V (2007) Cellulose, hemicelluloses, lignin and ash content of some organic materials and their suitability for use as paper pulp supplements. Biores Technol 98:296–301. https://doi.org/10.1016/j.biortech.2006.01.007

Vishtal A, Retulainen E (2014) Boosting the extensibility potential of fibre networks: a review. BioResources. 9:7951–8001. https://doi.org/10.15376/biores.9.4.7951-8001

Walker LC (2001) Dynamic mechanical spectroscopy of paper. Thermochim Acta 367:407–414. https://doi.org/10.1016/S0040-6031(00)00666-3

Wen C, Yuan Q, Liang H, Vriesekoop F (2014) Preparation and stabilization of d-limonene Pickering emulsions by cellulose nanocrystals. Carbohyd Polym 112:695–700. https://doi.org/10.1016/j.carbpol.2014.06.051

Wright T, Ali AM, Bechtold T (2020) Surface coated cellulose fibres as a biobased alternative to functional synthetic fibres. J Clean Prod 275:123857. https://doi.org/10.1016/j.jclepro.2020.123857

Zhang Z, Wang X, Gao M, Zhao Y, Chen Y (2020) Sustained release of an essential oil by a hybrid cellulose nanofiber foam system. Cellulose 27:2709–2721. https://doi.org/10.1007/s10570-019-02957-1

Zhang B, Bu X, Wang R, Shi J, Chen C, Li D (2021) High mechanical properties of micro fibrillated cellulose/HDPE composites prepared with two different methods. Cellulose 28:5449–5462. https://doi.org/10.1007/s10570-021-03885-9

Zhou S, Tashiro K, Hongo T, Shirataki H, Yamane C, Ii T (2001) Influence of water on structure and mechanical properties of regenerated cellulose studied by an organized combination of infrared spectra, X-ray diffraction, and dynamic viscoelastic data measured as functions of temperature and humidity. Macromolecules 34:1274–1280. https://doi.org/10.1021/ma001507x

Zhu T, Guo J, Fei B, Feng Z, Gu X, Li H, Zhang S (2020) Preparation of methacrylic acid modified microcrystalline cellulose and their applications in polylactic acid: flame retardancy, mechanical properties, thermal stability and crystallization behavior. Cellulose 27:2309–2323. https://doi.org/10.1007/s10570-019-02931-x